university of groningen

Physics-based Modeling and Control of a Heat Pump for District Heating

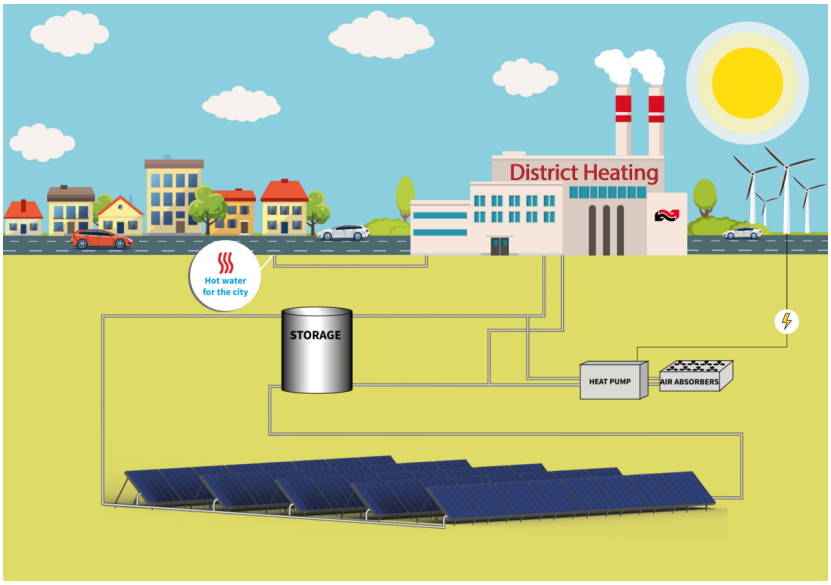

Ard de Reus, S2737477

Research Project Industrial Engineering and Management

First Supervisor: Prof. Dr. J.M.A. Scherpen
Second Supervisor: Prof. Dr. C. de Persis

First Daily Supervisor: Dr. J.M. Martinez
Second Daily Supervisor: Dr. M. Cucuzella

January 31, 2022

Abstract

Energy systems such as district heating systems require that different forms of energy can easily be converted into one another. A heat pump is a device which is able to achieve this, by converting electric energy into thermal energy. This is executed by means of the heat pump cycle, containing a compressor, condenser, valve and evaporator. In this thesis, the physics behind the cycle and its components are investigated, and written out in a dynamical model. The dynamical model couples a low temperature heat source to a district heating network via the heat pump cycle. It describes the dynamic behavior of the heat pump, based on the pressure of the refrigerant in the different components. One the one hand, this approach simplifies complex state-of-the-art physical models that are incompatible to couple in district heating context. On the other hand, it provides advanced physical detail in comparison to simplified heat pump models that were already developed for district-heating cases. Eventually, the physics-based modeling approach is verified through simulation, and design of a state feedback controller after linearization.

Contents

List of Figures

List of Tables

Nomenclature

Q	Heat transfer	W
W	Work	J
P	Pressure	Pa
T	Temperature	^oC
U	Internal energy	J
s	Entropy	J/K
h	Enthalpy	J
v	Specific volume	m^3/kg
D	Diameter tube	m
α	Heat transfer coefficient	W/m^2K
ρ	Density	kg/m^3
$\dot{m}$	Mass flow	kg/s
$\dot{Q}$	Heat transfer rate	J/s
L	Length of tube	m
C_p	Specific heat	J/kgK
A	Surface	m^2
v	flow velocity	m/s
V_c	volumetric displacement	m^3/s
V	volume	m^3
R	gas constant	$m^3Pa/Kmol$
ω	shaft speed	rev/s
A_v	Valve opening	m^2
γ	Fraction substance quality	
n	polytropic coefficient	
C_v	Orifice coefficient	

Subscripts:

g	gas
l	liquid
sh	superheated vapor
w	wall
r	refrigerant
dh	district heating
gs	ground source
i	inside

1 Introduction

As the Paris agreements require, energy systems should evolve toward zero-emission systems. Hence, humanity needs to rely more frequently on renewable energy sources like wind and solar instead of traditional fossil sources like oil and gas. Due to this transition, new challenges arise for designing energy systems.

For instance, due to increasing generation of electricity from wind and PV, flexibility on the demand side is required (Fischer and Madani (2017)). For both it holds that the energy demands are not always in line with it: it is beyond human control when the sun will shine and the wind will blow. This requires that generated energy should easily be stored, to be converted later on in a form that is desired. For instance, it should be possible to trade electricity for heat and vice versa. To deal with this flexibility problem, energy hubs were developed to increase optimal usage of energy resources. Energy hubs are multi-energy system which make it possible to convert one kind of energy form into another (Sadeghi et al. (2019)) Specifically, modern energy hubs are containing a set of interfaces between different energy systems which in turn embrace their own converters, transmission and distribution infrastructure (Sadeghi et al. (2019))

In the context of these energy hubs, there are several different options to convert different forms of energy into each other. A common demand is to convert electrical energy or fuel into thermal energy to satisfy heat demand. A device which is able to do so, is a *heat pump*. By means of electric power a heat pump is able to absorb thermal energy from a source and convert it into thermal energy which can be used for consumer purposes. Examples of common heat pumps are air source heat pumps (ASHP) and ground source heat pumps (GSHP). Generally speaking, it is shown that heat pumps offer the best solution for transforming the residential heat sector towards reduced CO2-emissions (Fischer and Madani (2017)). Besides, they will offer the required flexibility to satisfy demands whenever coupled to thermal storage (Fischer and Madani (2017)).

A schematic representation of a heat pump used in an energy hub is shown in figure 5. In this model, it can be seen that different resources of energy are converted and stored. The inputs are electricity and natural gas; the outputs are electricity and heat. The energy hub is able to switch over between different forms by use of a combined heat and power unit (CHP), heat pump (HP), electricity storage unit (ESU) and thermal storage unit (TSU) (Cao et al. (2020)). These four devices make the proposed scheme a powerful tool in overcoming the flexibility challenge.

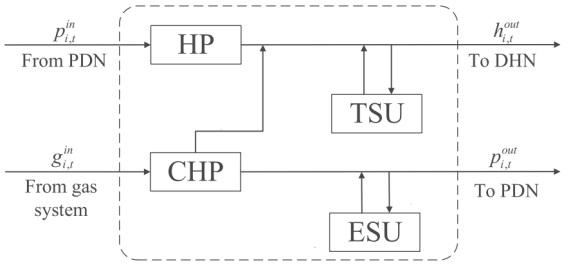

Fig. 1: Energy hub (Cao et al. (2020))

Energy hubs can be implemented effectively in a larger context of energy networks, to which multiple users and resources can be connected. An example of this is District Heating (DH), which comprises a network of insulated pipes which transports heated fluid, carrying thermal power from heating stations (producers) towards clusters of consumers within a neighborhood, town center or city (Lund et al. (2014)). Multiple sources of heat are delivering the required thermal energy, instead of a single power plant. The sources that are used, are decentralized energy hubs in which different types of energy are exchanged (Li et al. (2019)). Hence, in the context of district heating, an integrated energy approach needs to be taken to fulfill customer needs. Specifically, electrification of heating devices have created integrated energy distribution systems which harness multiple energy resources in urban areas. In this research, I will consider a central device used in this context: a heat pump. In the following chapter, I will introduce this device in its context, after which I will deliver the general outline for this thesis.

2 Research Context

Among multiple objectives, the main control function of a heat pump in DH-context is often to supply thermal energy to meet certain comfort requirements (Fischer and Madani (2017)). Several studies have already been done to the working of these devices in district heating systems (Fischer et al. (2017), Pedersen et al. (2011), Baniasadi et al. (2019), Klyapovskiy et al. (2018)). However, these authors focused on the DH-system or energy hubs as a whole, simplifying the heat pump to a certain extent. In this research I aim to deliver a detailed model of a heat pump, which can be integrated for DH and energy hub purposes. The final model should describe dynamic behavior and should be suitable for control purposes, to be eventually integrated into a larger context. In this section, I will first elaborate on an actual DH-context in which a heat pump is required (section 2.1). Afterwards, I will go into the state of the art of heat pump models (section 2.2), and the contribution I will make in this thesis (section 2.3).

2.1 District Heating

For this research, a specific DH case in which a heat pump is required will be investigated. A recent model of a DH-system is delivered by Machado et al. (2021), who proposed a comprehensive nonlinear ODE-based thermo-hydraulic model of a district heating system featuring several heat producers, consumers and storage devices. In this approach, each consumer and producer is connected with a tube to the district heating network, through which a cold or hot stream of a heat exchanger is flowing (Machado et al. (2021)). This is visualized in figure 2, in which $P_{pr,i}$ is the thermal power injected by a producer, and q_i the volumetric flow of water going through the DH-system.

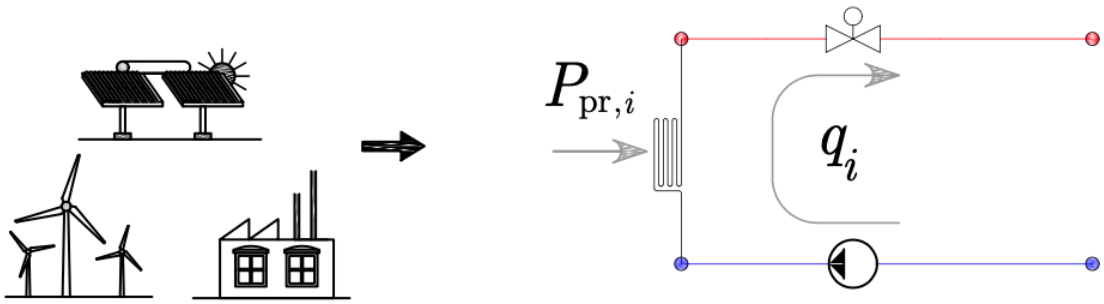

Fig. 2: Heat injection in a DH-system (Machado et al. (2021))

This model of Machado has been extended by Schiffer and Krishna (2021), who presented a multi-energy microgrid which is composed of an electrical and thermal system, connected via heat pumps. Schiffer and Krishna (2021) proposed that the dynamics of the thermal production itself need to be modeled as well, and hence take already into account some components of the heat pump itself. They explain that an heat pump is composed of an evaporator, a

compressor, a condenser and an expansion valve. The compressor is driven by a Permanent Magnet Synchronous Motor (PMSM), which makes it able to drive the heat pump at different speeds. In literature, this is also known as a *Variable Speed Heat Pump (VSHP)*, of which Kim et al. (2014) provided a detailed explanation. Schiffer and Krishna (2021) used this model to provide a heat supply for the DH-system. Assuming that the evaporator of the HP injects a heat flow to a pipe that has an inlet and an outlet through which cold and how water flows, thermal power can be injected to the district heating system. Subsequently, Schiffer and Krishna (2021) hereby proposed that a heat-pump model could be used to model the heat production in the DH approach of Machado as well (Schiffer and Krishna (2021)).

However, in doing so, Schiffer and Krishna (2021) only provided a simplified model of a heat pump model. The model solely includes temperature changes which the heat pump delivers to the DH-system, resulting from the shaft speed ω of the PMSM motor (Schiffer and Krishna (2021)) Unless that this input-output relationship is true (Kim et al. (2014), Vargas and Parise (1994)), it is a simplified manner of describing the dynamics of a heat pump in a larger context. Hence, this approach could be deepened, to gain advanced insights in the dynamics between producer and the district heating system.

In order to improve detail for the model of (Schiffer and Krishna (2021)), and supply the district heating model of Machado et al. (2021), a dynamical model for a heat pump will be developed in this thesis. This model can eventually be used to investigate the dynamic response in the DH-models of both Krishna & Schiffer and Machado. Eventually, this heat pump model could be used to perform stability and passivity analysis in further research, on both the individual component as well as the entire energy hub.

Besides that the model needs to have specific modeling and control characteristics, the model to be developed will be *physics-based*. This is advantageous for the scope of this research, since it gives freedom to couple all different components of the heat pump system. It provides an approach to go as much into detail as is desired, and to simplify where necessary. This is significantly different from approaches like Mahdavi and Braslavsky (2020) and Cao et al. (2020), who already impose some demands on the system beforehand and make their simplifications on basis of requirements. This thesis will start at the physics, and views the challenge of integration only at last. When starting at the physics, all dynamic responses between inputs and output can be taken into account. Next to level of detail, this provides flexibility to adapt the model later on to the context of integration. As Fischer et al. (2017) explains it, this approach entails that the heat pump is considered as individual physical agent, and only afterwards is interpreted from a perspective of (in)direct control.

Another interesting perspective that can be embraced in heat pump research, is to come up with a port-hamiltonian formulation of a heat pump model. This would deliver a new perspective on heat pump modeling and integration and opens up the opportunity for advanced analysis and simulation (van der Schaft (2006)). Unless that this topic is beyond the main scope of this research, a preliminary introduction of it is given in the discussion, for further research.

2.2 Heat Pumps

A broad overview of the integration of heat pumps in energy hubs and smart grids is given by Fischer et al. (2017), who compared different control approaches for variable speed air source heat pumps in integrated systems. Fischer et al. (2017) explained that certain input and control decisions are changing the behavior of the pump. For instance, the amount of fluid that needs to be heated and the type and amount of fluid that is used in the heat pump cycle itself, are influencing the thermal output and efficiency of the pump unit. Fischer et al. (2017) visualized the heat pump and its components in figure 3:

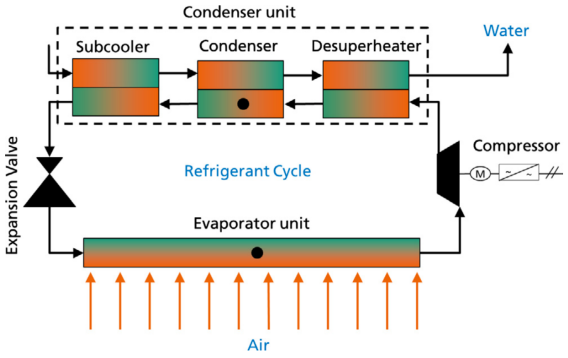

Fig. 3: Simplified representation of an air source heat pump (Fischer et al. (2017))

To integrate this into a broader context, Pedersen et al. (2011) provided an approach which aims at predicting the amount of power which is needed to maintain a specific control volume at a given pre-set temperature. The control volume considered is a domestic living room, viewed in terms of thermal resistance. However, in this dynamic model the heat pump is only viewed from an input-output relation in which the pump itself is formulated in terms of its Coefficient of Performance (COP) (Pedersen et al. (2011)). Baniasadi et al. (2019) is integrating a heat pump in a thermal management system with thermal storages. However, again the heat pump is only taken into account as energy conversion unit with a certain COP (Baniasadi et al. (2019)). Similarly, the approach of Péan et al. (2019) simplified the dynamics of the refrigeration cycle itself in order to investigate the integrated context. Hence, since these state-of-the-art models research on heat pump integration do not provide any detail on a physical level, we will further zoom in on physical modeling of refrigeration cycles.

Technically speaking, many of the commercial heat pump systems that are fulfilling a task as Schiffer and Krishna (2021) described, are comprised of a single-stage vapor compression cycle as shown figure 3. This vapor compression cycle is also widely known as a refrigeration cycle or heat pump cycle. It consists of a single evaporator and condenser, absorbing and rejecting heat. Furthermore, it is driven by a compressor, and completed by an expansion valve to make the cycle go round. Later on, this components will all be discussed extensively. However, the basic principle behind this cycle is that vapor is compressed and expanded in this cycle to transport thermal energy (Chua et al. (2010)). A novel way to boil the refrigerant in the evaporator of the heat pump, is to heat it by means of a low temperature heat source, such as geothermy. In that case, the heat pump is called a geothermal heat pump or ground source heat pump (GSHP) (Chua et al. (2010)). The advantage of this technology is that the temperature of the earth is quite constant. This makes low-temperature heat pumps one

of the most efficient, comfortable, and quiet heating and cooling technologies available today (Chua et al. (2010)). Another common way to heat the refrigerant is by means of cold air (Fischer et al. (2017)). Both GSHP's and ASHP's require the refrigerant to be of a very low temperature in the evaporator, such that it will boil very quickly [1].

Furthermore, from a district-heating perspective, there are other novel low-temperature heat sources that could be used to deliver the required thermal energy for the heat pump. For instance, solar heating systems can be used to deliver heat. For city-based DH-systems, a large solar plant could be placed outside a city and through well-insulated tubes deliver a heated stream to the DH-system. Another promising option would be to use waste water from industrial processes or cooling process in industrial buildings. However, in all these options it could be that there is mismatch between the requirement of thermal energy and the availability (for instance, in the winter there is less solar power available, but heat is required). Hence, this requires detailed dynamic performance investigation and planning of the entire district heating system, as well as a heat pump specifically (Lund et al. (2014)).

A promising approach for a heat pump model is delivered by Kim et al. (2014), who presented a dynamical model of a variable speed heat pump in a commercial building that responds to dynamic load control. In figure 4, the visual representation of their model is shown. The model is basically composed of four components: (1) a variable speed drive connected to the electrical grid and the compressor, (2) a variable speed heat pump connected to the compressor (3) which influences the experimental room temperature (4). For now, it is not relevant to explain all symbols and components in detail: enough is to understand that the integrated approach of Kim et al. (2014) is able to satisfy thermal requirements by power control. The system is controlled by means of a power/temperature controller which regulates the speed of the variable speed drive, powering the compressor. In their paper, Schiffer and Krishna (2021) referred to this model to integrate a heat pump in DH-context.

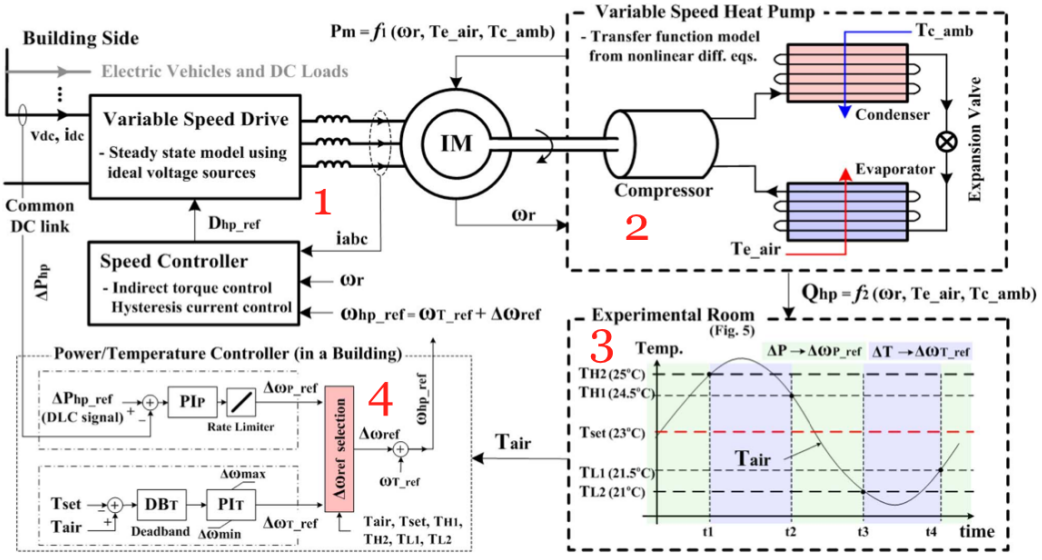

Fig. 4: Simplified schematic diagram VSHP-model (Kim et al. (2014))

[1] Due to its relatively low saturation temperature at low pressure.

The model of Kim et al. (2014) is designed to deliver a perspective on an integrated heat pump for control purposes. It includes several different components of a VSHP in combination with a supply of electric power and thermal demands. Kim et al. (2014) formulated the dynamics of the VSHP in the following way:

$$P_m = k_\omega \omega_r + k_c T_{c,amb} + k_e T_{e,air} + k_{offset} \tag{1}$$

In which the output is the required compressor mechanical power (P_m), and the inputs are the shaft speed (ω), the condenser ambient temperature ($T_{c,amb}$) and evaporator air temperature ($T_{e,air}$). The temperatures hence are the temperatures of the substances that are injecting or absorbing heat in or from the system.

The coefficients k_ω, k_c, k_e and k_{offset} are determined by using a polynomial multiple regressive algorithm. According to Kim et al. (2014), the linear dependencies of this equation are in line with the VSHP models presented by B.P. Rasmussen (2006) and He (1996). However, in these papers and in Zhang et al. (2014) and Vargas and Parise (1994) it is shown that refrigeration cycles are showing highly complex non-linear behavior. Hence, the linear representation of the heat pump of Kim et al. (2014) is leaving out detail to understand the physics that are going on in the heat pump itself. Hence, the approach of Kim et al. (2014) does not give an account for the dynamic behavior of a refrigeration cycle.

Nevertheless the models presented by Vargas and Parise (1994) and He (1996) are delivering some detailed insights in dynamic heat pump behavior. However, they are not yet fully suitable for DH-implementation. Vargas and Parise (1994) presented a model composed of conservation equations, in time-derivative form, as well as fluid property equations, resulting in a set of differential and algebraic equations that describe the system response to variations in the ambient thermal load. However, these equations do not provide one clear state equation through which the heat pump dynamics can be understood. Besides, this model was used for air conditioning of a single room, and was not tested as integrated heat pump in a larger system. This also holds for He (1996), who delivered a lumped-parameter heat-pump model, describing the actuating inputs and performance outputs as a set of high-order, non linearly coupled equations. However, the focus of He is to validate the physics of his model, rather then to deliver a model suitable to integrate it into a larger system. Nevertheless, the models of He (1996) and Vargas and Parise (1994) can be extrapolated and simplified in order to obtain a model which is compatible with the DH-models of Machado et al. (2021) and Schiffer and Krishna (2021).

2.3 Contributions

This thesis delivers a mathematical model of a heat pump that can be used for integration in a DH-system. This requires that an aggregated model-for-control is developed, describing the dynamic behavior of the heat pump. A heat pump is a complex physical device possessing non-linear behavior. Hence, a lumped-parameter approach will be undertaken to model all components, aiming to describe dynamic behavior in terms of ordinary differential equations (ODE's). On the one hand, previous literature presented us with partial differential equations and highly complex models (B.P. Rasmussen (2006), He (1996)). However, from a control perspective, these models are challenging to linearize and control. On the other hand, there are models which are simplifying much of the dynamics that happen between different components in a heat pump (Kim et al. (2014), Vargas and Parise (1994)). Those models are not satisfactory in delivering a level of detail in which the heat pump dynamics can be adjusted and recomputed to achieve desired results.

Hence, the goal of this research is to deliver a model which delivers an adequate description of the complex dynamics of a refrigeration cycle, maintaining the simplicity to be suitable for control purposes.

After having developed such a model based on the thermodynamic physics going on in the refrigeration cycle, it needs to be shown that this model is suitable for control purposes. Hence, a steady-state analysis will be carried out to research the equilibrium of the model. Subsequently it will be shown that the dynamical model is stable and usable for control design. Eventually, a state feedback system will be designed for the model.

Accordingly, the thesis will be structured in the following way. In chapter 3 the heat pump system will be described in more detail, explaining the different components. It will be explained which parts are within the scope of this research, and which are excluded. Afterwards, in chapter 4 the physics of the different components is elaborated on. The physical interpretation subsequently will lead to the ODE's that will describe the dynamic behavior of the heat pump. Then, in chapter 5 the dynamical model will be used for steady state analysis and simulation, and eventually design of a state feedback controller.

In chapter 6 the obtained physical model and its implications will be discussed and reflected upon. The contributions of the research will be highlighted, accompanied by the limitations and opportunities for further research. Specifically, a preliminary discussion of a port-hamiltonian formulation of the model will be given, suitable for further research. Finally, in chapter 7, I will round off with a conclusion.

3 System Description

In this chapter, the different components of the heat pump will be introduced and schematically modeled (section 3.1). The first details regarding the physics of the refrigeration cycle will be provided (section 3.2), which will be modeled in detail in chapter 4 afterwards. Additionally, it is discussed which variables are suitable for describing the heat pump cycle mathematically, by zooming in on the energy balances in the condenser and evaporator (section 3.3) .

3.1 System Design

In this project, a heat pump system should be analyzed which is able to convert electric energy into thermal energy. The heat pump absorbs heat from a low temperature heat source, and delivers it to a district heating network. The heat pump system should figure as intermediary in order to satisfy thermal requirements.

The system that will be subject of research is represented in figure 5. The aim of the system is to deliver heat from the low temperature heat source (A) to the district heating network (H) by means of a heat pump cycle (C,D,E,F). The heat transfer between the source, heat pump cycle and district heating system occurs in the heat exchangers, outlined in red. Specifically, in the light of previous explanations, it can be said that this figure is what is behind $P_{pr,i}$ in figure 2 (page 4), and that the heat pump cycle is the same as what was explained by figure 3 (page 6).

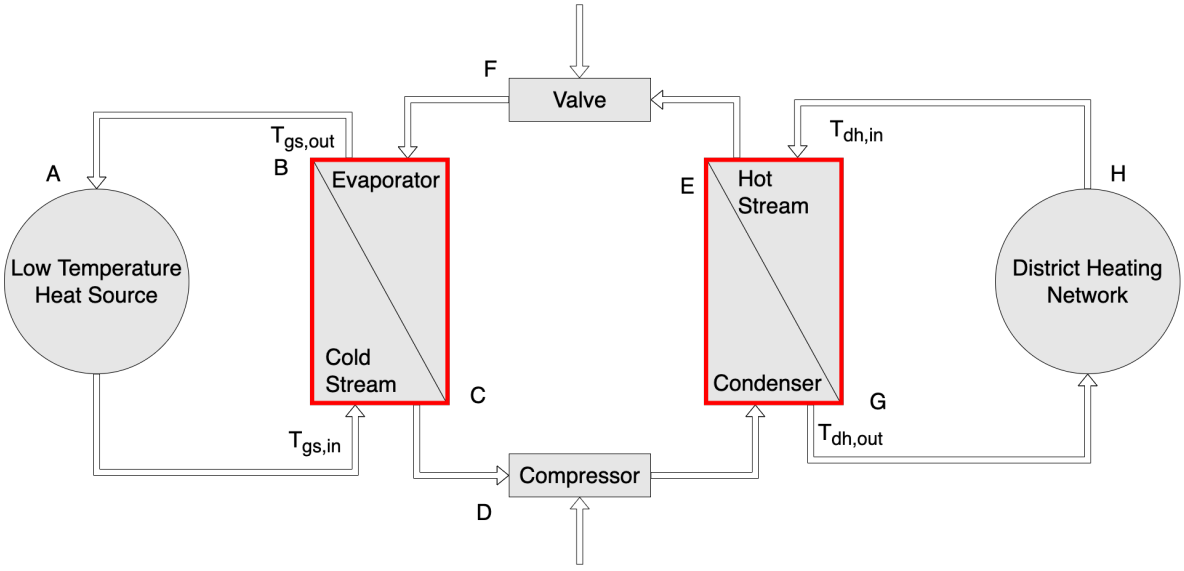

Fig. 5: Schematic system model

The different components can be explained in the following way:

A: Low temperature heat source A low temperature heat source can be air or a heat source which delivers water with a constant temperature. As explained, this stream can be supplied by a ground heat source, or other novel ways such as waste water or a solar plant. For this research the general assumption is made that the source delivers water. Accordingly, it needs to be ensured that the source fluid has sufficiently high temperature ($T_{gs,in}$) to let the refrigerant evaporate through heat conduction. Due to the heat conduction, the source fluid will loose temperature and will leave the heat exchanger with temperature $T_{gs,out}$.

B: Cold stream heat source It is a assumed that ground source delivers a fluid through perfectly-insulated pipes to a heat exchanger. The heat exchanger ensures that heat conduction can take place between the stream of the source and the refrigerator in the refrigeration cycle, such that the refrigerant can evaporate.

C: Evaporator In the evaporator, the refrigerant changes phase due to the heat conduction through the heat exchanger. The input of the evaporator will be a liquid, and the output a saturated vapor (Vargas and Parise (1994), Cengel et al. (2019)). The refrigerant used in this research, will be refrigerant R134a, which is a common refrigerator used in heat pump applications (Cengel (2008)).

D: Compressor The compressor compresses the saturated vapor delivered by the evaporator into a superheated vapor. The compression process should increment the temperature of the sufficiently, such that the vapor can eventually deliver heat to the district heating system. The compressor can be manipulated by changing the shaft speed ω, which makes the heat pump a VSHP. By adjusting this input, the volumetric flow in the entire heat pump cycle can be adjusted according to requirements.

E: Condenser The superheated vapor enters the condenser and looses heat through heat conduction with the heat exchanger. In the condensation process, the refrigerant changes phase from superheated vapor to saturated vapor, and saturated liquid at last.

F: Valve The valve completes the refrigeration cycle by lowering the pressure on the fluid. By doing so, the saturation temperature of the refrigerant is reduced drastically as well, and the liquid obtains the properties to boil again in the evaporator.

G: Hot stream district heating The second heat exchanger of the system ensures that heat is absorbed by the fluid stream going to the district heating system. Heat is conducted through the tube wall from the heat pump refrigerant to the district heating stream.

H: District heating network Water is coming in from the DH-system with temperature $T_{dh,in}$, and is heated up by the heat exchanger connected to the heat pump cycle. After the water flowing through the heat exchanger is heated, the heated fluid is transported towards the district heating network, in which it can deliver heat to e.g. households or buildings. The temperature of the water $T_{dh,out}$ hence should be increased sufficiently to meet comfort requirements.

An example of the system of figure 5 is shown in figure 6 (Baniasadi et al. (2019)):

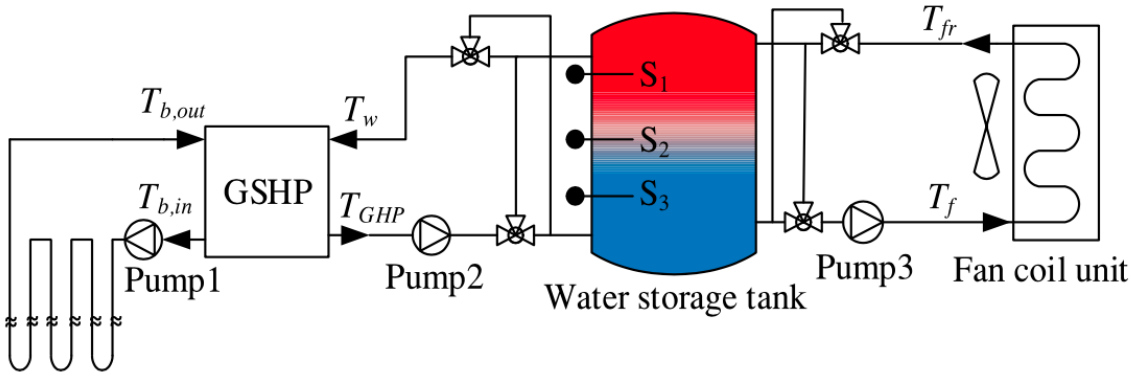

Fig. 6: Schematic of a thermal energy system (Baniasadi et al. (2019))

This is a schematic representation of an experimental thermal energy system in of the Smart Energy Laboratory of the Edith Cowan University, Joondalup, Western Australia. The set-up is similar to figure 5. The heat pump (Ground Source Heat Pump) is coupled to a ground heat source, which delivers heat by stream T_b to the heat pump, delivering thermal energy to flow T_w, being part of a system of flows and storages. The heat pump model of figure 5 that will be studied in this thesis can be seen as similar to this experimental set-up.

3.2 Refrigeration Physics

As previously mentioned, a device that extracts heat from low-temperature reservoir and rejects or transfers it to a high-temperature reservoir is called a refrigerator (or heat pump). The cycle followed by this device or system is called a *refrigeration cycle* (Kaushik et al. (2017)). The aim is to reject or extract heat from a selected space, and to supply heating or cooling to another space. In the context of this research project, the aim will be to extract heat from source A and to supply it to goal H (see figure 5). Basically, a refrigeration cycle exists of four processes (Cengel et al. (2019)):

1. Isentropic compression in a compressor
2. Constant-pressure heat rejection in a condenser
3. Throttling in an expansion device
4. Constant-pressure heat absorption in an evaporator

These steps are visualized in figure 7.

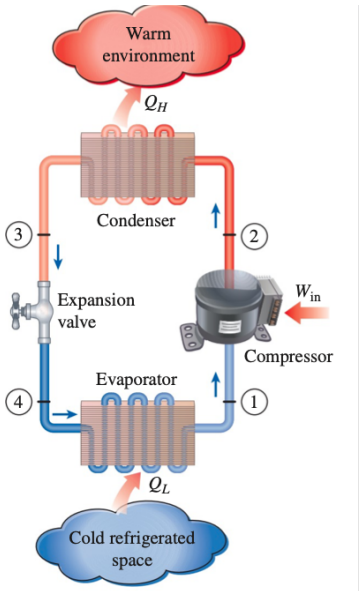

Fig. 7: Ordinary heat pump cycle (Cengel et al. (2019))

Accordingly, the general energy balance for this cycle corresponds to:

$$Q_L + W_{in} = Q_H \tag{2}$$

In which Q_L is the amount of heat injected into the system at the evaporator, W_{in} the work done by the compressor, and Q_H the heat rejected by the condenser. Unless that this equation is a steady state balance equation, it provides a general understanding of an overarching energy balance for the refrigeration cycle. However, as explained, in this research a dynamic modeling approach in undertaken. In this thesis, the refrigeration cycle will be seen as an ideal-vapor compression cycle. This assumes that there are no losses to the environment and that there is no fluid friction. Generally, heat pump cycles can be described with the graphs of figure 8:

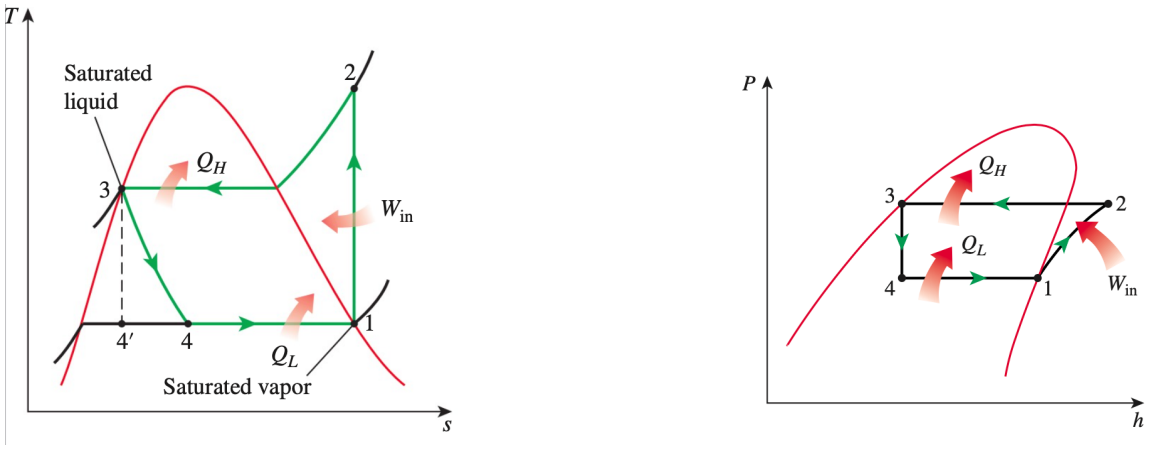

Fig. 8: Temperature-Entropy and Pressure-Enthalpy diagrams of a refrigeration cycle (Cengel et al. (2019))

The graphs of figure 8 describe the physical phase-changing process the refrigerant undergoes in the heat pump cycle. In between 1 and 2, the fluid changes phase from saturated vapor to a superheated vapor, due to compression. Between 2 and 3, the refrigerant condensates and heat transfer to the external environment takes place. In this process, the pressure of the refrigerant is assumed to be uniform (Vargas and Parise (1994), He (1996)). Afterwards, in between 3 and 4, the condensated saturated liquid goes through a throttling valve which is used as expansion device. This ensures that the fluid has the right saturation temperature to be able to boil when going through the evaporator in between 4 and 1. After these processes, the cycle repeats.

3.3 Energy Balances

To establish a lumped-parameter dynamical model of the compressor, condenser, valve and evaporator, the physics of each component needs to be quantified at first. To ensure that explanation will not be done twice, only the condenser will be described in the following sections. The refrigeration cycle as explained can be reversed, after which it will work as air conditioning system instead as heat pump. Therefore, the evaporator and condenser are in fact similar components, only subject to a different positions. Hence, whenever the condenser is mentioned, it can be assumed that the evaporator exhibits the same properties but reversed.

The conservation of energy will be taken into account in describing the flow of the refrigerant through the different components (MacArthur and Grald (2021), He (1996)). It can be assumed that the potential and kinetic energies are zero in the tubes of the system, which implies that the differential form of the energy balance equation 2 of all components can be expressed in the following way (Cengel (2008)):

$$\delta Q - \delta W = \delta U \tag{3}$$

In which the change in internal energy corresponds to the work and heat added to the system (equation 2). However, it needs to be taken into account that:

$$\delta Q = Tds \qquad \text{and} \qquad \delta W = PdV$$

Or in other words, the quantity $(\frac{\delta Q}{T})$ corresponds to a differential change in the property entropy. The development of the entropy throughout a process hence can be evaluated by integrating this quantity $(\frac{\delta Q}{T})$. Unless that entropy is hard to measure directly, it quantifies the measure of total energy present in a system.[2] The other measure of energy is work (δW). If work is applied to a gas, it can be described as the differential change in volume times the pressure (Cengel (2008)).

Accordingly, equation 3 can be rewritten as:

$$Tds = dU + Pdv \tag{4}$$

[2] This will reflected upon later in this thesis as well when the port-hamiltonian formulation is discussed.

Which is a derivation of the *Gibbs equation*:

$$H = U + PV \tag{5}$$

In which it can be seen that the definition of enthalpy (H) is the sum of the pressure-volume product and the internal energy. Thus, enthalpy can also be written down in terms of temperature and entropy (equation 4). However, both equations 4) and 5 describe the internal energy in a system.

Equation 4 can also be understood as the product of the differential change in entropy at constant temperature is equal to the enthalpy of the system. It is a way to describe the energy balance in a system. It implies that the rate of change of internal energy (dU) is dependent upon the change of entropy (dS) and specific volume (dv), assuming uniform pressure (P) and temperature (T). Consequently, equation 4 can be rewritten in form of the Maxwell relations (Cengel et al. (2019)):

$$\left(\frac{\delta T}{\delta v}\right)_s = -\left(\frac{\delta P}{\delta s}\right)_v \tag{6}$$

Which implies that the partial derivative of the temperature with respect to the volume of a system is equal to the negative partial derivative of the pressure with respect to the entropy. This relation represents the thermodynamic potential of a system. Hence, it can be rewritten as the thermodynamic equation of state (Cengel (2008)):

$$\left(\frac{dh}{dP}\right)_T = v - T\left(\frac{dv}{dT}\right)_P \tag{7}$$

This analysis reveals how we should view the internal dynamics of the condenser: The rate of change of enthalpy with respect to the pressure is equal to the rate of change of the specific volume with respect to the temperature. Assuming uniform pressure and temperature in the condenser and evaporator tubes, it can be seen that the enthalpy and specific volume are the quantities that vary and are dependent upon the pressure and temperature.

Since we will assume uniform pressure along the condenser and evaporator (see figure 8, p.16), the energy balance of the refrigerant flowing through the tubes can be viewed in the following way (He (1996)):

$$\text{Energy Balance:} \quad \frac{d(\rho h - P)}{dt} = \frac{4}{D_i}\alpha_i(T_w - T_r) \tag{8}$$

In which:

v: specific volume

h: enthalpy of the refrigerant

P: pressure of the refrigerant

λ: friction coefficient

D_i: the inner diameter of the tube

T_r: bulk temperature of the refrigerant

T_w: temperature of the tube wall

α_i = heat transfer coefficient

The left hand side of equation 8 has the same structure as equation 4, describing the changes in internal energy in terms of pressure, specific volume (density) and enthalpy.

The partial derivatives considered by He (1996) for these variables along the axis of flow (z) will not be taken into account. Why it is chosen to do so, is further elaborated on in section 4.1. However, the refrigerant is in continuous movement throughout the tube and changes density due to phase change. Therefore, the mass flow inside the tube will also vary. Accordingly, the mass balance for the tube also needs to be taken into account:

$$\text{Mass Balance:} \quad \frac{\delta \rho_{in} u_{in}}{\delta t} = \frac{\delta \rho_{out} u_{out}}{\delta t} \tag{9}$$

Eventually, the aim of the dynamic model of the condenser is to capture the amount of heat transferred to the district heating network. Hence, an adequate state variable needs to be chosen such that the heat transfer and temperature can be monitored and finally controlled. If we take a closer look at the discussed energy balances and diagrams, it can be seen that the enthalpy can be computed based on the pressure (figure 8). Combining this with Gibbs equation 5, the specific volume can consequently be computed. And if the pressure, enthalpy and density are all known, the saturation temperature can be computed via the thermodynamic equation of state. Therefore, it can be concluded that as an independent state variable for the dynamics inside the condenser and evaporator the pressure of the refrigerant could be chosen. Based on this, the remaining unknown variables can be derived from it. Hence, the following dependencies will be used in this thesis:

$$\rho = \rho(P) \qquad T = T(P) \qquad h = h(P)$$

In the following chapters, pressure will be used as the independent variable to describe the state of the refrigerant flowing through the cycle. Having this state variable will make it possible to describe the dynamics of the system in ODE's instead of partial differential equations: dependencies upon temperatures, densities and internal energies can be traced back to pressure states and hence will simplify the computations for dynamic equations.

4 Problem Formulation

The aim of this chapter is to deliver an aggregated model describing the dynamics of the heat pump. Aggregated entails that all components are incorporated, such that the model easily can be coupled to a district heating system. First, the dynamics of the condenser and evaporator will be considered. It will be explained how a lumped-parameter approach will suffice in simplifying the dynamics in the tube and the heat exchanger (section 4.1). Afterwards, the dynamics of the refrigerator inside the condenser and evaporator tubes will be discussed and modeled (section 4.2). This will result in a state-space model for the heat transfer in the condenser and evaporator (section 4.3). Additionally, the dynamics of the compressor (section 4.4) and valve (section 4.5) will be discussed, after which a modular model (section 4.6) and an aggregated model (section 4.7) for the heat pump are presented.

4.1 A Lumped-parameter Approach

In the approach taken in this research, the condenser tube will be viewed as a single component. This so-called lumped-parameter approach simplifies the model in light of its final purpose for implementation in a district heating system. A discretization of the entire condenser, such as done by MacArthur and Grald (2021) is left out of consideration. An first alternative is provided by He (1996), who suggests a moving-interface approach, in which the tubes are lumped into different nodes to obtain more accurate equations for the refrigerator dynamics. However, this approach still requires that the tubes are discretized along the axis of flow. A second alternative is the approach of Vargas and Parise (1994), where an average of the qualities of the substance inside the tube was taken, which approximates and simplifies the properties of the substance in the tubes. This is the approach that will be used in this thesis as well. Since we are aiming to compute the performance of the system for heat transfer to the district heating system, the full dynamics of the refrigerant in the tubes can be left out of scope. But this means that we have to take into account that the way we describe the dynamics inside the condenser and evaporator will not have maximum accuracy, due to simplification purposes. This can be visualized in figure 9:

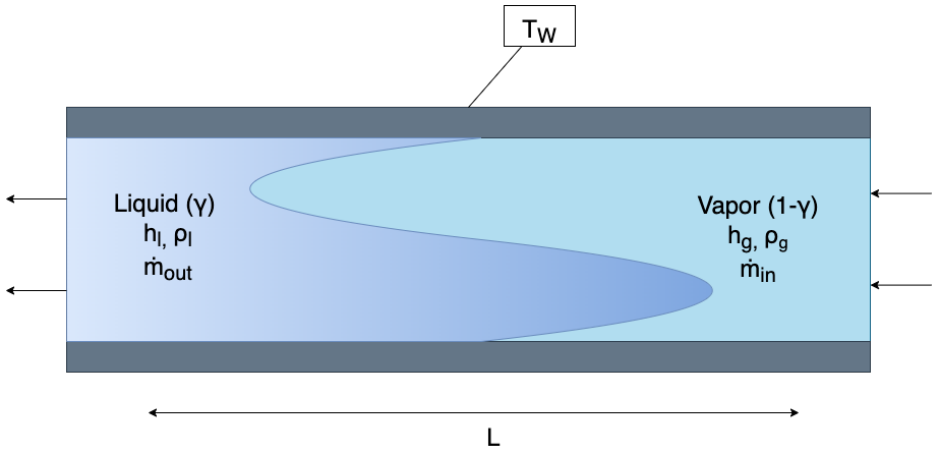

Fig. 9: A lumped parameter schematic representation of the condenser

Figure 9 is a schematic representation of the condenser, consisting of two different sections. The right section consists of superheated vapor coming in. Section 2 consists of saturated liquid going out. For both two sections, the enthalpy and density are computed, and averaged afterwards by means of the fraction γ. By separating the tube in two parts, heat transfer properties can be estimated more adequately then taking it as one component.

The heat transfer when phase change occurs through the heat exchanger generally depends upon the enthalpy of vaporization h_{fg} (Cengel (2008)):

$$\dot{Q} = \dot{m} h_{fg} \tag{10}$$

And hence both the enthalpies of the saturated liquid and vapor need to be taken into account for averaging the enthalpy. Vargas uses the following equation to do so for the condenser:

$$h_{cond} = x h_{vapor} + (1 - x) h_{liquid} \tag{11}$$

In which x is the approximated space-averaged quality of the different substances inside the evaporator. We will do the same, replacing x with γ.

For the evaporator, a similar approach can be taken. However, it needs to be taken into account that the evaporator contains a different mixture than the condenser. As can be seen in figure 8 (p.16), the superheated section (point 2), differs from the enthalpy of the saturated vapor. Vargas and Parise (1994) is taking this into account by using the same equation as equation 11, but taking into account that x might be different. On the one hand, this neglects the fact the the condenser actually exists out of three substances: superheated vapor, saturated vapor and saturated liquid. On the other hand, this significantly simplifies the model. Hence, in this thesis the middle will be sought by modelling both the evaporator and condenser with only two phases. However, for the condenser one of those phases will be seen as superheated vapor instead of saturated vapor, improving the approximated average. For the remainder of this thesis, for both heat exchangers the variables γ_1 and γ_2 will be introduced to account for the quality of the substance inside.

4.2 Refrigerator Dynamics

With all explained physics, we now are able to formulate the dynamics of the internal energy in the condenser and evaporator as visualized in figure 9. As can be seen in equation (8) (p.18), changes in enthalpy, pressures and specific volume throughout the tube need to be taken into account. Specifically, the differential change of total energy in the tube is equal to:

$$\frac{d(\rho h)}{dt} - \frac{dP}{dt} \tag{12}$$

However, as explained, since the tube is averaged on basis of two sections, the internal energy should be averaged. For the evaporator this would result in the following equation:

$$\left(\frac{d(\rho_l h_l)}{dt}(1 - \bar{\gamma}) + \frac{d(\rho_g h_g)}{dt}\bar{\gamma} \right) - \frac{dP}{dt} \tag{13}$$

These internal energy changes consequently will affect the heat transfer rate towards the tube wall (He (1996)). Besides, as shown in equation (9), the dynamics inside the tube are determined by the properties of the mass flow coming in and out. The mass balance of the tube hence needs to be incorporated in the energy balance of the tube, and can be formulated in the following way:

$$\frac{\delta \rho u}{\delta t} = \dot{m}_{in} h_{in} - \dot{m}_{out} h_{out} \tag{14}$$

Together with the conduction to the outer stream this makes up for the following energy balance equation:

$$AL_1 \left(\frac{d(\rho_l h_l)}{dt}(1-\bar{\gamma}) + \frac{d(\rho_g h_g)}{dt}\bar{\gamma} - \frac{dP}{dt} \right) = \dot{m}_{in} h_{in} - \dot{m}_{out} h_{out} + \alpha_{i1} D_i L_1 (T_w - T_r) \tag{15}$$

where:

A: cross-sectional area of flow

L_1: the length of the tube

$\bar{\gamma}$: the fraction of gas in the tube

ρ: the density of the substance

h: the enthalpy of the substance

$\dot{m}$: massflow at the entrance or exit of the tube.

α: heat transfer coefficient between refrigerant and tube wall

D: diameter of the tube

T: Temperature

The subscripts l and g are corresponding to either liquid or gas properties of the refrigerant, and in and out to inlet and outlet properties. For the temperature the subscripts w and r are referring to either the wall of refrigerant.
The left hand side of this equation defines the energy inside the evaporator tube[3], partly being liquid and partly being vapor. The total change in this energy is equal to the right hand side, which corresponds to the energy going in and out, and conduction.

As introduced in section 3.3, pressure is chosen as the independent variable in this equation. The density, enthalpy and temperature of the refrigerant are computed on basis of this. According to Cleland (1992), the properties of refrigerant R134a can be estimated using curve-fit polynomials. The relationships that will be used in order to account for the pressure-enthalpy-density-temperature relations in this research, are stated in Appendix I. A similar thing is done

[3] As explained previously, this equation generally both holds for the evaporator and condenser, taking into account some detailed differences. These will be discussed in the next section.

by Hauschild et al. (2020), who estimate the properties of water by use of polynomials when modeling a district heating network.[4].

In order to use equation (15), some substitutions will be made to reach an equation with one state variable. The mass flow ($\dot{m}$), which is a variable of interest for the dynamics of the evaporator and condenser, will be written down as $\rho A v$. This makes it possible to consider the mass flow as product of a changing density, dependent on the pressure, and control input flow velocity (which will be discussed later on). Simultaneously, the time derivative of the product of density and enthalpy (left hand side of (15)), needs to be computed. Accordingly, all densities, enthalpies and refrigerant temperatures need to be written down depending upon pressure as independent variable (as explained on page 19). Following upon equation 13, this is be mathematically represented in the following steps:

$$\left(\frac{\partial \rho_l}{\partial P}\frac{\partial h_l}{\partial P}\right)\frac{\partial P}{dt} + \left(\frac{\partial \rho_g}{\partial P}\frac{\partial h_g}{\partial P}\right)\frac{\partial P}{\partial t} - \frac{\partial P}{\partial t} \tag{16}$$

$$= \left(\frac{\partial \rho_l}{\partial P}\frac{\partial h_l}{\partial t}\right) + \left(\frac{\partial \rho_l}{\partial t}\frac{\partial h_l}{\partial P}\right) + \left(\frac{\partial \rho_g}{\partial P}\frac{\partial h_g}{\partial t}\right) + \left(\frac{\partial \rho_g}{\partial t}\frac{\partial h_g}{\partial P}\right) - \frac{\partial P}{\partial t} \tag{17}$$

$$= \left(\rho_{l(P)}\frac{\partial h_{l(P)}}{\partial t}\right) + \left(h_{l(P)}\frac{\partial \rho_{l(P)}}{\partial t}\right) + \left(\rho_{g(P)}\frac{\partial h_{g(P)}}{\partial t}\right) + \left(h_{g(P)}\frac{\partial \rho_{g(P)}}{\partial t}\right) - \beta \tag{18}$$

With β as pressure constant, and in which ρ and h can be substituted by polynomial estimation and its time derivatives by the derivatives of the respective polynomials.

Consequently, $\left(\frac{d(\rho_l h_l)}{dt}(1-\bar{\gamma}) + \frac{d(\rho_g h_g)}{dt}\bar{\gamma} - \frac{dP}{dt}\right)$, can be replaced with equation 18, and the mass flow $\dot{m}$ in $\dot{m}_{in}h_{in} - \dot{m}_{out}h_{out}$ can be written in terms of $\rho A v$. This results in the following form of (15):

$$\begin{aligned} &AL_1\left(\left(\left(\rho_{l(P)}\frac{\partial h_l}{\partial t}\right) + \left(h_{l(P)}\frac{\partial \rho_l}{\partial t}\right)\right)(1-\bar{\gamma}) + \left(\left(\rho_{g(P)}\frac{\partial h_g}{\partial t}\right) + \left(h_{g(P)}\frac{\partial \rho_g}{\partial t}\right)\right)(\bar{\gamma}) - \beta\right) \\ &= \rho_{in,l(P)}h_{in,l(P)}Av - \rho_{out,g(P)}h_{out,g(P)}Av + \alpha_{i1}D_iL_1(T_w - T_{r(P)}) \end{aligned} \tag{19}$$

This equation can be applied to both the condenser and evaporator. However, in the condenser the density and enthalpy need to be estimated on basis of the properties of superheated vapor instead of saturated vapor. This will be accounted for by introducing the factor η, which is an estimation for the difference between both vapor phases.

Since the polynomials of Cleland (1992) involve higher-order terms dependent upon saturation temperature instead of pressure, it is chosen to use the same method, but not the resulting polynomials. The `MATLAB` command `polyfit` (Mathworks (2021)) is used to fit second-order polynomials to the data of Appendix II.

[4] the port-hamiltonian approach they use, will be briefly introduced later on in section 6.3

Hence, all enthalpy, density and temperature terms depending upon pressure can be substitution by a corresponding polynomial or its derivative. The polynomials can be found in Appendix I. This table is a numerical representation of the graphs of figure 8 for refrigerant R134a.

4.3 Tube Walls

As can be seen in figure 5 and equation (19), the properties of the refrigerant are partly dependent upon the wall temperature T_w, which is the body between the flow coming from either the ground heat source or the district heating system and the heat pump cycle. Hence the wall temperature is a state variable representing the conduction between the outer stream and the heat pump cycle. This is visualized in figure 10, which represents the entire heat exchanger for the evaporator:

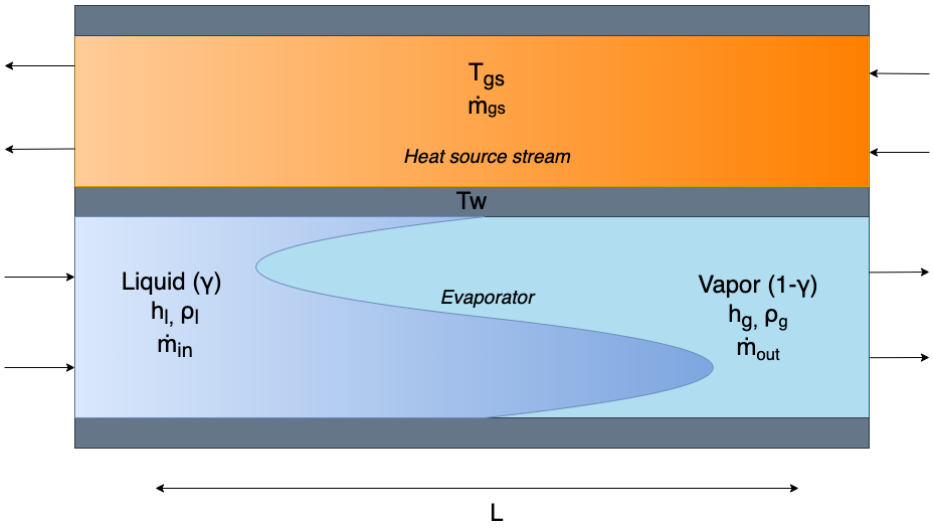

Fig. 10: A lumped parameter schematic representation of the entire heat exchanger with heat source stream and evaporator

Hence, the wall temperature is subject to conduction by transferring heat from the flows at either side. Heat transfer in a heat exchanger can be described by the following equation (Cengel (2008)):

$$\dot{Q} = UA\Delta T \tag{20}$$

In which the heat transfer rate $\dot{Q}$ depends upon the heat transfer coefficient U, the surface size and the temperature difference ΔT between the two fluids. However, since we are interested in the temperature of the wall, conduction from two sides need to be taken into account:

$$\dot{Q} = U_r A_w \Delta T_r + U_{gs} A_w \Delta T_{gs} \tag{21}$$

Accordingly, the temperature of the wall is defined by the this heat transfer rate (Cengel (2008)) and the heat capacity of the material:

$$\Delta T_{wall} = \frac{\dot{Q}}{C_{p,w}\rho_w} \tag{22}$$

$$\Delta T_{wall} = \frac{U_r A_w \Delta T_r + U_{gs} A_w \Delta T_{gs}}{C_{p,w}\rho_w} \tag{23}$$

Which makes the energy balance of T_w for the evaporator the following when rearranging terms:

$$C_{p,w}\rho_w A_w \frac{dT_w}{dt} = D_i \alpha_i (T_r - T_w) + D_{gs}\alpha_{gs}(T_{gs} - T_w) \tag{24}$$

In which:

$C_{p,w}$: the specific heat of the wall

ρ_w: the density of the wall

A_w: the surface which is subject to heat transfer

T_w: the temperature of the wall

D_i: the diameter of the condenser/evaporator tube

α_i: the heat transfer coefficient of the heat pump tube wall

α_{gs}: the heat transfer coefficient of the tube wall of the outer flow

T_r: the temperature of the refrigerant

T_{gs}: the temperature of the flow coming from the ground source.

In this equation, the left hand corresponds to changes of the temperature of the tube wall. The right hand side determines this change, based on the temperature differences with the heating fluid and the refrigerant.

Following the same line of computation, the flow coming in from the ground heat source T_{gs} is affected from one side by the temperature of the wall. Besides, since the temperature of the flow coming from the ground heat source is dependent upon the input temperature, which needs to be taken into account as well:

$$C_{P,w}\rho_w \frac{dT_{gs}}{dt} = C_p \dot{m}_{gs}(T_{in} - T_{dh}) + D_{gs}\alpha_{gs}(T_{gs} - T_w) \tag{25}$$

In which T_{in} is the inlet temperature of the mass flow $\dot{m}_{gs}$ coming from the ground heat source. From a control perspective, these can either be specified beforehand or viewed as disturbance.

Accordingly, the state equation for the evaporator ($\dot{x}_e$) can be described by taking the temperature dynamics of the flow coming from the source, the tube wall and the dynamics of the refrigerant, dependent upon pressure. This can be described by using equation (15), (24) and (25) all together:

$$\begin{bmatrix} \dot{P}_e(t) \\ \dot{T}_w(t) \\ \dot{T}_{gs}(t) \end{bmatrix} = \begin{bmatrix} \frac{\rho_{in}(_{Pe})h_{in}(_{Pe})Av - \rho_{out}(_{Pe})h_{out}(_{Pe})Av + \alpha_{i1}D_iL_1(T_w - T_r(_{Pe})))}{AL_1\left(\left(\left(\rho_l(_{Pe})\frac{\partial h_l}{\partial t}\right) + \left(h_l(_{Pe})\frac{\partial \rho_l}{\partial t}\right)\right)(1-\bar{\gamma}) + \left(\left(\rho_g(_{Pe})\frac{\partial h_g}{\partial t}\right) + \left(h_g(_{Pe})\frac{\partial \rho_g}{\partial t}\right)\right)(\bar{\gamma}) - \beta\right)} \\ \frac{D_i\alpha_i(T_r(_{Pe}) - T_w) + D_{gs}\alpha_{gs}(T_{gs} - T_w)}{C_{P,w}\rho_w A_w} \\ \frac{C_p\dot{m}_{gs}(T_{in} - T_{dh}) + D_{gs}\alpha_{gs}(T_{gs} - T_w)}{C_{P,w}\rho_w v} \end{bmatrix} \tag{26}$$

For the condenser, the same computation steps can be undertaken. Hence, I will show the computations, without explaining in detail what corresponds to what.

The energy balance consisting of the properties of superheated vapor and liquid is shown in equation 27:

$$AL_1\left(\frac{d(\rho_{sh}h_{sh})}{dt}(1-\bar{\gamma}) + \frac{d(\rho_l h_l)}{dt}\bar{\gamma} - \frac{dP}{dt}\right) = \dot{m}_{in}h_{in} - \dot{m}_{out}h_{out} + \alpha_{i1}D_iL_1(T_w - T_r) \tag{27}$$

Which undergoes the same substitutions as the evaporator:

$$\begin{aligned} &AL_1\left(\left(\left(\rho_{sh}(_P)\frac{\partial h_{sh}}{\partial t}\right) + \left(h_{sh}(_P)\frac{\partial \rho_{sh}}{\partial t}\right)\right)(1-\bar{\gamma}) + \left(\left(\rho_l(_P)\frac{\partial h_l}{\partial t}\right) + \left(h_l(_P)\frac{\partial \rho_l}{\partial t}\right)\right)(\bar{\gamma}) - \beta\right) \\ &= \rho_{in,sh}(_P)h_{in,sh}(_P)Av - \rho_{out,l}(_P)h_{out,l}(_P)Av + \alpha_{i1}D_iL_1(T_w - T_r(_P)) \end{aligned} \tag{28}$$

Subsequently, the condenser heats up the tube wall between the district heating system and the refrigerant:

$$C_{P,w}\rho_w A_w\frac{\delta T_w}{dt} = D_i\alpha_i(T_r(_{Pc}) - T_w) + D_{dh}\alpha_{dh}(T_{dh} - T_w) \tag{29}$$

In which T_{dh} is the temperature of the flow in the district heating system:

$$C_{P,w}\rho_w v\frac{\delta T_{dh}}{dt} = C_p\dot{m}_{dh}(T_{dh} - T_{in}) + D_{dh}\alpha_{dh}(T_{dh} - T_w) \tag{30}$$

Accordingly, the state space equation for the condenser ($\dot{x}_c$) is the following:

$$\begin{bmatrix} \dot{P}_c(t) \\ \dot{T}_w(t) \\ \dot{T}_{dh}(t) \end{bmatrix} = \begin{bmatrix} \frac{\rho_{in,sh}(P_c)h_{in,sh}(P_c)Av - \rho_{out,l}(P_c)h_{out,l}(P_c)Av + \alpha_{i1}D_iL_1(T_w - T_r(P_c))}{AL_1\left(\left(\left(\rho_{sh}(P_c)\frac{\partial h_{sh}}{\partial t}\right) + \left(h_{sh}(P_c)\frac{\partial \rho_{sh}}{\partial t}\right)\right)(1-\bar{\gamma}) + \left(\left(\rho_l(P_c)\frac{\partial h_l}{\partial t}\right) + \left(h_l(P_c)\frac{\partial \rho_l}{\partial t}\right)\right)(\bar{\gamma}) - \beta\right)} \\ \frac{D_i\alpha_i(T_r(P_c) - T_w) + D_{dh}\alpha_{dh}(T_{dh} - T_w)}{C_{P,w}\rho_w A_w} \\ \frac{C_p\dot{m}_{dh}(T_{in} - T_{dh}) + D_{dh}\alpha_{dh}(T_{dh} - T_w)}{C_{P,w}\rho_w v} \end{bmatrix} \tag{31}$$

In section 4.6, this equation will be coupled with the other components. However, they will need an introduction first as well. Besides the evaporator and condenser, there are two other components that make up the heat pump cycle: the compressor and expansion valve. In order to couple these components to equations (26) and (31), they should deliver inputs for the input and output of the refrigerator state equation in the form of total energy delivered to the component. This corresponds to $\dot{m}h$, which is shown in this equation as $h(_{Pc})Av$. However, in the upcoming sections, there will often solely be referred to $\dot{m}$ in order to simplify the physical understanding of the coupling procedure: the compressor delivering a flow to the condenser and the valve to the evaporator.

4.4 Compressor

In the context of refrigeration modeling, compressors are often modeled as steady-state components (Nyers and Stoyan (1994), He (1996), Vargas and Parise (1994), Zhang et al. (2014)). However, this entails that the dynamics inside the compressor are not taken into account. Nevertheless, I will very briefly consider two dynamical approaches to reflect if it indeed is the right decision to not model them dynamically when modeling a heat pump cycle.

A dynamic approach was presented by Xie and Bansal (2000) and Ndiaye and Bernier (2009). Xie and Bansal (2000) describe the compressor on basis of ten differential equations, having multiple equations for all different parts of the compressor. Ndiaye and Bernier (2009) simplify this by dividing the compressor in 6 different parts, and delivering a useful equation regarding the energy conservation of the refrigerator going through the shell of the compressor:

$$\frac{d\rho_c h_c}{dt}V_f = \dot{m}_{suc}h_{suc} - \dot{m}_2 h_2 + \dot{Q}_c + \dot{Q}_{ch} + \frac{dP_{suc}}{dt}V_f \tag{32}$$

In which the right hand consists of inlet and outlet terms, heat delivered from the motor ($\dot{Q}_c$) and crankcase ($\dot{Q}_{ch}$) to the refrigerator, and the pressure variation over time.

This equation could possibly be implemented in equations (26) and (31). However, this would require to specify compressor properties elaborately and would increase the difficulty of the entire heat pump model. An advantage would be that the accuracy of the compressor dynamics would be increased. However, Xie and Bansal (2000) already point out that a compressor in fact can be understood in the following way:

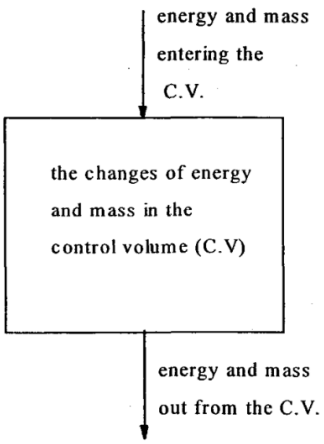

Fig. 11: Schematic of control volume modeling for compressor (Xie and Bansal (2000))

Complementary, Rasmussen et al. (2002), He (1996) and Vargas and Parise (1994) argue that the dynamics of response of the compressor are an order-of-magnitude faster then heat exchangers, and that hence quasi-steady-state conditions should be assumed (He (1996))[5]. This entails that we should model the steady state input-output relation as shown in figure 11, without going in too much detail about what dynamics happen inside the box. This is what will be done in this research as well, to simplify the compressor model. Nevertheless, the approaches of Ndiaye and Bernier (2009) and Xie and Bansal (2000) are promising in delivering more detail in the future.

Hence, a general steady state equation for the compressor is introduced to account for its behavior. Heat addition by compressor components will be neglected, being negligible in comparison to heat transfer in other parts of the heat pump cycle. The equation for polytropic compressor (A polytropic processes means that $Pv^n = \text{constant}$.) work is the following (Cengel et al. (2019), A.S.H.R.A.E. (2008)):

$$W_{comp} = \frac{nRT}{n-1}\left[\left(\frac{P_2}{P_1}\right)^{(n-1)/n} - 1\right] \tag{33}$$

The general equation for the mass flow going through the compressor is:

$$\dot{m} = V_c \omega \rho \tag{34}$$

Combining equation (33) and (34), we obtain the following equation:

$$\dot{m}_c = V_c \omega \rho_{sh}\left[\left(\frac{P_2}{P_1}\right)^{(n-1)/n} - 1\right] \tag{35}$$

[5] (He (1996)) explains that the rise time of the compressor speed for a step change of 10Hz is less than 4 seconds, and 100ms for the valve. In contrast, the response of the heat exchangers of the evaporator and condenser is more than 40 seconds!

In which n is the polytropic coefficiënt, C_c the compressor coefficient, V_c the volumetric displacement in m^3, ω_c the revolutions per second of the compressor, p_{in} and p_{out} the inlet and outlet pressure in Pa. ρ_{sh} is the density of the outlet superheated vapor. As previously done, this density is formulated in terms of pressure. The resulting massflow consequently needs to be divided by the flow area and density of the superheated vapor, to obtain the flow velocity. This value can then be substituted in equations (26) and (31) to compute the pressure state. However, the value η of the superheated vapor is harder to estimate compared to the saturated vapor and liquid sections. As mentioned, this value is outside the pressure-enthalpy curve of figure 8, an estimation needs to be made for the difference between the properties of the saturated and superheated vapor. He (1996) makes this estimation based on the compressor efficiency η_c:

$$h_{out} = \frac{h_{out} - h_{in}}{\eta_c} + h_{in} \tag{36}$$

Accordingly, as explained in section 4.2 curve fitting will be used for estimating the density, enthalpy and temperature of the saturated liquid and vapor, which subsequently can be used as the inlet and outlet conditions used for the compressor. The properties of the superheated vapor will be adjusted by compressor multiplier η.

4.5 Valve

The working of the can be derived from Bernoulli's equation (Li (2012)). As valve an electronic expansion valve is chosen, since it can by controlled by electronic signals. Liquid refrigerant flowing through expansion valve can be modeled through the following equation (He (1996)):

$$\dot{m}_v = C_v A_v \sqrt{(\rho_v)\,(P_c - P_e)} \tag{37}$$

In which C_v is the orifice coefficient, A_v the the opening area, ρ_v the density of the refrigerant and ΔP The pressure drop across the refrigerant. In this case, A_v can be adjusted to achieve the desired $\dot{m}_v$.

Important to mention is that no work is applied when the fluid flows through the expansion valve. Only the pressure is lowered, usually accompanied by a large temperature drop (Cengel (2008)).

Similar to the compressor, the resulting mass flow consequently needs to be divided by the flow area and density of the liquid, to obtain the flow velocity. This value can then be substituted in the state equation for the condenser to compute the pressure state.

4.6 Modular Model

In order to study and control the behavior of the entire refrigeration cycle, all explained components are put together. The final goal is to regulate $T_{dh,out}$, and to satisfy the heat demand of the district heating network. After investigating the dynamics of all different components, figure 5 can be adjusted to obtain figure 13:

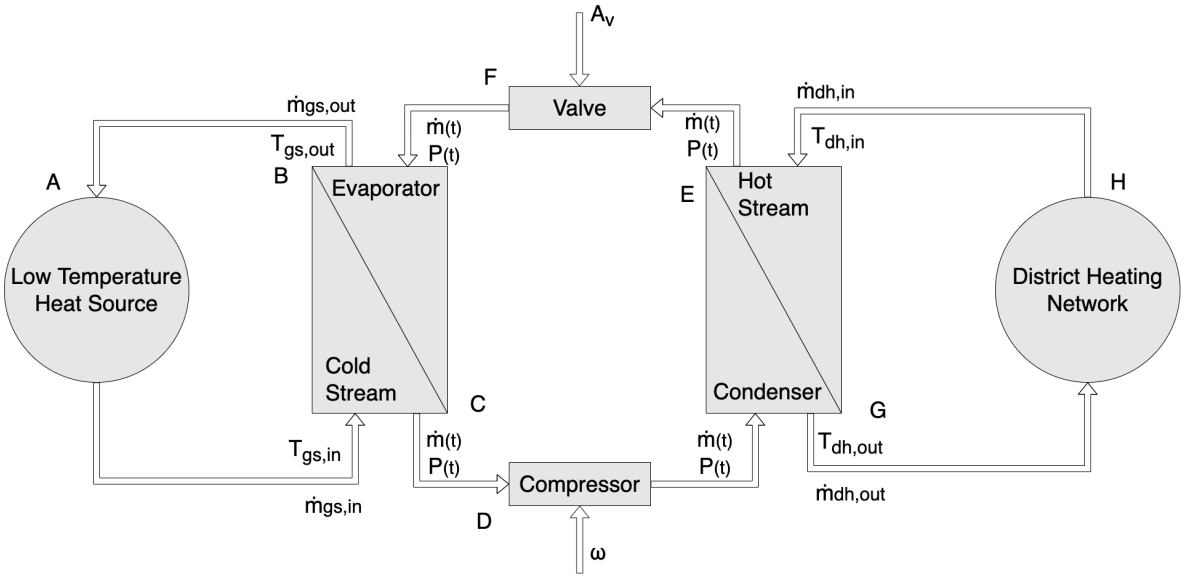

Fig. 12: Schematic system model with variables

In which $(P_c, T_{w,dh}, T_{dh}, P_e, T_{w,gs}, T_{gs})$ are the state variables of the system, representing the properties of the heat pump cycle. Accordingly, for equations (31) and (26) the control inputs are the flow velocity coming from the compressor and the flow going through the valve. Hence, whenever we view all components separately the following dynamical model can be composed:

$$\dot{x}_e = f_e(x_e, \dot{m}_{gs}, \dot{m}_e) \tag{38}$$

$$\dot{x}_c = f_c(x_c, \dot{m}_{dh}, \dot{m}_c) \tag{39}$$

$$\dot{m}_e = C_v A_v \sqrt{(\rho_v)\,(P_{in} - P_{out})}) \tag{40}$$

$$\dot{m}_c = V_c \omega \rho_{sh} \left[\left(\frac{P_2}{P_1} \right)^{(n-1)/n} - 1 \right] \tag{41}$$

In which the control inputs for this representation are the following: ω_c is the compressor shaft speed, $\dot{m}_{dh}$ the mass flow coming in from the district heating system, A_v the opening of the expansion valve, and $\dot{m}_{dh}$ the mass flow coming from the low temperature heat source.

Graphically, this can visualized by the block diagram shown in figure 13:

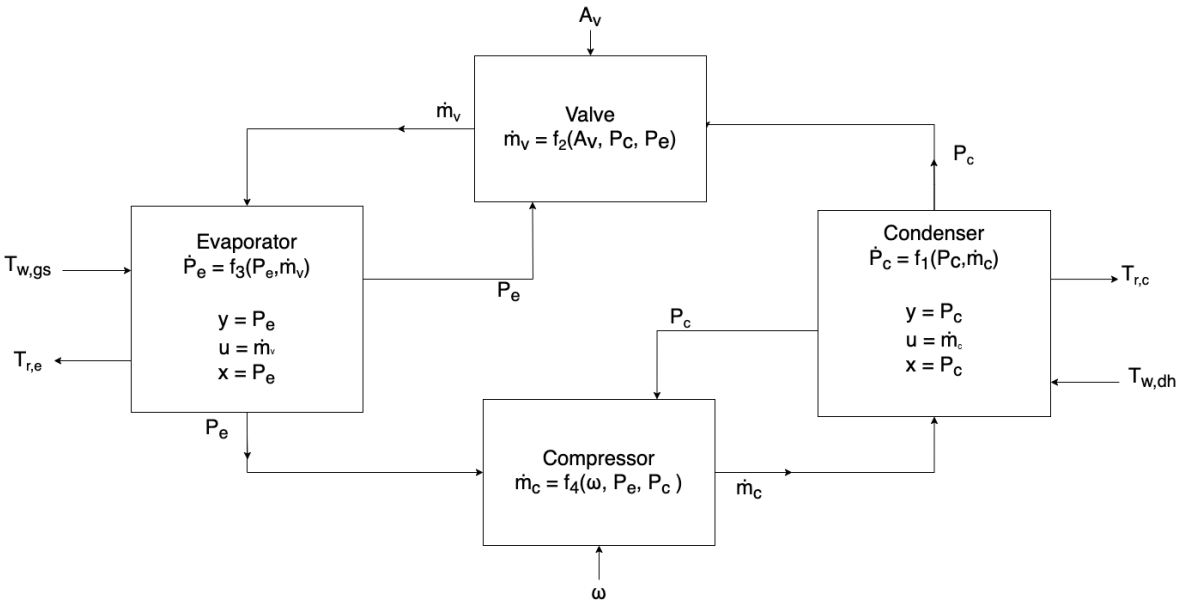

Fig. 13: Block diagram heat pump cycle

In figure 13, f_1 corresponds to equation 39, f_2 to 40, f_3 to 38, and f_4 to 41. the dynamics of the four different components are separated clearly, and this can also be understood as a modular model. The reason for incorporating this model is to deliver a start for further research. A modular approach separates the dynamics of the different components, which makes it able to view the components separately from a port-hamiltonian perspective. This will be briefly introduced in the discussion (section 6.3).

4.7 Aggregated Model

To design a controller for the developed system, it would be beneficial to integrate the parts even more and to obtain as less state space equations as possible. Hence, we will continue by aggregating the modular model further on. As mentioned in the introduction, one of the goals of this research project is to deliver a model which easily can be implemented in district heating modelling. Hence, the model will be aggregated by merging the valve and compressor model in the condenser and evaporator.

As shown on the previous page, the compressor and valve deliver inputs for the more complex evaporator and condenser. Besides, the order of magnitude of the dynamics of the valve and compressor is larger. If we view them as steady-state, they can simply be substituted in the state equations for the condenser and evaporator to achieve a more unified model.

Accordingly, the following two equations make up for the entire refrigeration loop: equation 42 (x_c) for the condenser and 43 (x_e) for the evaporator

$$\begin{bmatrix} \dot{P}_c(t) \\ \dot{T}_w(t) \\ \dot{T}_{dh}(t) \end{bmatrix} = \begin{bmatrix} \frac{V_c\omega_c(\rho_{sh}(P_c))\left(\left(\frac{P_e}{P_c}\right)^{(n-1)/n}-1\right)h_{in,sh}(P_c) - C_vA_v\sqrt{(\rho_l(P_c))\,(P_c-P_e)}h_{out,l}(P_c) + \alpha_{i1}D_iL_1(T_w-T_r(P_c))}{AL_1\left(\left(\left(\rho_{sh}(P_c)\frac{\partial h_{sh}}{\partial t}\right)+\left(h_{sh}(P_c)\frac{\partial \rho_{sh}}{\partial t}\right)\right)(1-\bar{\gamma})+\left(\left(\rho_l(P_c)\frac{\partial h_l}{\partial t}\right)+\left(h_l(P_c)\frac{\partial \rho_l}{\partial t}\right)\right)(\bar{\gamma})-\beta\right)} \\ \frac{D_i\alpha_i(T_r(P_c)-T_w)+D_{dh}\alpha_{dh}(T_{dh}-T_w)}{C_{P,w}\rho_wA_w} \\ \frac{C_p\dot{m}_{dh}(T_{in}-T_{dh})+D_{dh}\alpha_{dh}(T_{dh}-T_w)}{C_{P,w}\rho_wv} \end{bmatrix} \tag{42}$$

$$\begin{bmatrix} \dot{P}_e(t) \\ \dot{T}_w(t) \\ \dot{T}_{gs}(t) \end{bmatrix} = \begin{bmatrix} \frac{C_vA_v\sqrt{(\rho_l(P_e))\,(P_c-P_e)}h_{in,l}(P_e) - V_c\omega_c\rho_{in,g}(P_e)\left(\left(\frac{P_e}{P_c}\right)^{(n-1)/n}-1\right)h_{out,g}(P_e) + \alpha_{i1}D_iL_1(T_w-T_r(P_e))}{AL_1\left(\left(\left(\rho_l(P_e)\frac{\partial h_l}{\partial t}\right)+\left(h_l(P_e)\frac{\partial \rho_l}{\partial t}\right)\right)(1-\bar{\gamma})+\left(\left(\rho_g(P_e)\frac{\partial h_g}{\partial t}\right)+\left(h_g(P_e)\frac{\partial \rho_g}{\partial t}\right)\right)(\bar{\gamma})-\beta\right)} \\ \frac{D_i\alpha_i(T_r(P_e)-T_w)+D_{gs}\alpha_{gs}(T_{gs}-T_w)}{C_{P,w}\rho_wA_w} \\ \frac{C_p\dot{m}_{gs}(T_{in}-T_{dh})+D_{gs}\alpha_{gs}(T_{gs}-T_w)}{C_{P,w}\rho_wv} \end{bmatrix} \tag{43}$$

In these state space equations, it can be seen that the steady-state algebraic descriptions of the compressor and valve are substituted. In the condenser, the mass flow coming in was substituted by compressor equation 41 and the mass flow going out by valve 40. For the evaporator this was done vice versa.

Accordingly, this system has four control inputs (u^T):

$$u_1 = \omega_c \qquad u_2 = A_v \qquad u_3 = \dot{m}_{dh} \qquad u_4 = \dot{m}_{gs}$$

Given these inputs, sequentially $P(t)$, $T_w(t)$, $T_{dh}(t)$ and $T_{gs}(t)$ can be solved.

This results in the following dynamical model:

$$\dot{x} = F(x, u) \tag{44}$$

where

$$x = (x_e^T x_c^T) \quad \text{and} \quad u = (u^T)$$

In which x is the vector of state variables and u are the control variables. These equations will be the basis for the steady state analysis and feedback design of chapter 5.

5 Simulation & Control

In this chapter the dynamic model of section 4.7 will be subject of simulation and control design. This will verify the model and validate if it is stable for further integration and coupling. At first, we will further develop the model and aim to find a method through which the equilibrium of the dynamic model can be found (section 5.1). Afterwards, a steady state analysis will be carried out by using the model for a particular district heating case (section 5.2). Consequently, these parameters can be used for an open loop simulation (section 5.3). Finally, the model will be linearized around an equilibrium point (section 5.4), and state feedback controller will be designed for the system (section 5.5).

5.1 Forced Equilibria

Simpson-Porco (2018) provided a method to find equilibria for non-linear control affine systems. This can be of use for this research in particular to obtain the equilibria for the developed heat pump model. For Simpson-Porco (2018), this equilibrium determination is a method to investigate equilibrium-independent-dissipativity properties of a system, which can be used for the control of port-hamiltonian systems (Jayawardhana et al. (2007)). However, within the scope of this thesis we will not investigate system dissipativity, but only use the method of Simpson-Porco (2018) to transform the system to find an equilibrium.

Simpson-Porco (2018) describes that to obtain the equilibria $\bar{x}$ and $\bar{u}$ for the system:

$$\sum : \left\{ \dot{x}(t) = f(x(t)) + G(u(t)), \qquad y(t) = h(x(t)) + Ju(t) \right\} \tag{45}$$

with state $x(t) \in \chi := R^n$, input $u(t) \in \mathbb{R}^m$, there exists an equilibrium configuration $(\bar{u}, \bar{x}, \bar{y})$ that satisfies the following conditions:

$$0_n = f(\bar{x}) + G(\bar{u})$$

$$\bar{y} = h(\bar{x}) + J(\bar{u})$$

When $m < n$, The associated input equilibrium $\bar{u}$ is $-G^{-1}f(\bar{x})$. Let $G^{\perp} \in \mathbb{R}^{(n-m)n}$ be a full-rank left annihilator of G, such that $G^{\perp}$ satisfies $G^{\perp}G = 0$. Then, it follows that $\bar{x} \in \chi \mid G^{\perp}f(\bar{x}) = 0_{n-m}$ (Simpson-Porco (2018)). Accordingly, to find the set of assignable equilibrium states $(\bar{x})$ and corresponding inputs $\bar{u}$, $G^{\perp}$ needs to be found.

In order to find $G^{\perp}$, we first need to identify what $G(x)$ is for the heat pump model of this research. Hence, first the system of equations $F(x, u)$ needs to be transformed in the form $F(x, u) = f(x) + G(x)u$. This notation also will be helpful in particular when control design is performed.

Input matrix $G(x)$ is be a 6x4 matrix. Not all inputs apply to all states, and hence this matrix should have the following form:

$$G(x)u = \begin{bmatrix} \alpha_1 & \alpha_2 & 0 & 0 \\ 0 & 0 & 0 & 0 \\ 0 & 0 & \alpha_3 & 0 \\ \alpha_4 & \alpha_5 & 0 & 0 \\ 0 & 0 & 0 & 0 \\ 0 & 0 & 0 & \alpha_6 \end{bmatrix} \begin{bmatrix} \omega \\ A_v \\ \dot{m}_{dh} \\ \dot{m}_{gs} \end{bmatrix} \tag{46}$$

In which the symbolic variables correspond to the following equations:

$$\alpha_1 = \frac{V_c(\rho_{sh}(x1)) \left(\left(\frac{x_4}{x_1} \right)^{(n-1)/n} - 1 \right) h_{in,sh}(x1)}{AL_1 \left(\left(\left(\rho_{sh}(x1) \frac{\partial h_{sh}}{\partial t} \right) + \left(h_{sh}(x1) \frac{\partial \rho_{sh}}{\partial t} \right) \right) (1 - \bar{\gamma}) + \left(\left(\rho_l(x1) \frac{\partial h_l}{\partial t} \right) + \left(h_l(x1) \frac{\partial \rho_l}{\partial t} \right) \right) (\bar{\gamma}) - \beta \right)}$$

$$\alpha_2 = \frac{-C_v \sqrt{(\rho_l(x1))\,(x_1 - x_4)} h_{out,l}(x1)}{AL_1 \left(\left(\left(\rho_{sh}(x1) \frac{\partial h_{sh}}{\partial t} \right) + \left(h_{sh}(x1) \frac{\partial \rho_{sh}}{\partial t} \right) \right) (1 - \bar{\gamma}) + \left(\left(\rho_l(x1) \frac{\partial h_l}{\partial t} \right) + \left(h_l(x1) \frac{\partial \rho_l}{\partial t} \right) \right) (\bar{\gamma}) - \beta \right)}$$

$$\alpha_3 = \frac{C_p(T_{in} - x_3)}{C_{P,w} \rho_w v}$$

$$\alpha_4 = \frac{-V_c \rho_{in,g}(x4) \left(\left(\frac{x_4}{x_1} \right)^{(n-1)/n} - 1 \right) h_{out,g}(x4)}{AL_1 \left(\left(\left(\rho_l(x4) \frac{\partial h_l}{\partial t} \right) + \left(h_l(x4) \frac{\partial \rho_l}{\partial t} \right) \right) (1 - \bar{\gamma}) + \left(\left(\rho_g(x4) \frac{\partial h_g}{\partial t} \right) + \left(h_g(x4) \frac{\partial \rho_g}{\partial t} \right) \right) (\bar{\gamma}) - \beta \right)}$$

$$\alpha_5 = \frac{C_v \sqrt{(\rho_l(x4))\,(x_1 - x_4)} h_{in,l}(x4)}{AL_1 \left(\left(\left(\rho_l(x4) \frac{\partial h_l}{\partial t} \right) + \left(h_l(x4) \frac{\partial \rho_l}{\partial t} \right) \right) (1 - \bar{\gamma}) + \left(\left(\rho_g(x4) \frac{\partial h_g}{\partial t} \right) + \left(h_g(x4) \frac{\partial \rho_g}{\partial t} \right) \right) (\bar{\gamma}) - \beta \right)}$$

$$\alpha_6 = \frac{C_p(T_{in} - x_6)}{C_{P,w} \rho_w v}$$

Which corresponds with $F(x, u)$ if the following matrix for $f(x)$ is taken:

$$f(x) = \begin{bmatrix} \dfrac{\alpha_{i1} D_i L_1 (x_2 - T_r(_{x1}))}{AL_1 \left(\left(\left(\rho_{sh}(_{x1}) \frac{\partial h_{sh}}{\partial t}\right) + \left(h_{sh}(_{x1}) \frac{\partial \rho_{sh}}{\partial t}\right)\right)(1-\bar{\gamma}) + \left(\left(\rho_l(_{x1}) \frac{\partial h_l}{\partial t}\right) + \left(h_l(_{x1}) \frac{\partial \rho_l}{\partial t}\right)\right)(\bar{\gamma}) - \beta \right)} \\ \dfrac{D_i \alpha_i (T_r(_{x1}) - x_2) + D_{dh} \alpha_{dh} (T_{dh} - x_2)}{C_{P,w} \rho_w A_w} \\ \dfrac{D_{dh} \alpha_{dh} (x_3 - x_2)}{C_{P,w} \rho_w v} \\ \dfrac{\alpha_{i1} D_i L_1 (x_5 - T_r(_{x4}))}{AL_1 \left(\left(\left(\rho_l(_{Pe}) \frac{\partial h_l}{\partial t}\right) + \left(h_l(_{Pe}) \frac{\partial \rho_l}{\partial t}\right)\right)(1-\bar{\gamma}) + \left(\left(\rho_g(_{Pe}) \frac{\partial h_g}{\partial t}\right) + \left(h_g(_{Pe}) \frac{\partial \rho_g}{\partial t}\right)\right)(\bar{\gamma}) - \beta \right)} \\ \dfrac{D_i \alpha_i (T_r(x(4)) - x_5) + D_{gs} \alpha_{gs} (x_6 - x_5)}{C_{P,w} \rho_w A_w} \\ \dfrac{D_{gs} \alpha_g s (x_6 - x_5)}{C_{P,w} \rho_w v} \end{bmatrix} \tag{47}$$

Accordingly, $G^{\perp}$ can be formulated as 4x6 matrix containing symbolic variables, such that $G^{\perp}G$ can be computed.

$$G^{\perp} = \begin{bmatrix} a_{11} & a_{12} & a_{13} & a_{14} & a_{15} & a_{16} \\ b_{11} & b_{12} & b_{13} & b_{14} & b_{15} & b_{16} \\ c_{11} & c_{12} & c_{13} & c_{14} & c_{15} & c_{16} \\ d_{11} & d_{12} & d_{13} & d_{14} & d_{15} & d_{16} \end{bmatrix} \tag{48}$$

The resulting system of equations for $G^{\perp}G = 0$ can be computed, such that $a_{11} \dots d_{16}$ can be solved numerically with `MATLAB`.

However, the only feasible solution returned by `MATLAB` turns out to be $G^{\perp} = 0^{4\times 6}$, which is the trivial solution. This solution is inappropriate for further linearization and control design, since it lacks a physical interpretation. Due to time constraints, it was not possible to validate this further on and investigate if adjustments in the model would have led to different results when using the method of Simpson-Porco (2018). The practical implications and physical interpretations of this method for this specific heat pump case are too complex to investigate in full detail in this research.

However, the method of Simpson-Porco (2018) forced to write the system in $F(x) = f(x) + G(x)u.$ form, which will be used in the following chapter to carry out open loop steady state analysis and design state feedback, such that an equilibrium nevertheless can be found.

5.2 Steady State Analysis

For a steady state analysis of the developed heat pump model, properties of a heat pump and district heating system deployed in Saanich, Canada are used (Duquette et al. (2016)). Duquette et al. (2016) focuses on physical modeling of a district heating system, and hence provides values that are realistic to use for the variables of the heat pump model of this thesis. This grid is a DH-grid which uses effluent water for heating and cooling purposes, by means of distributed heat pumps. But before the substitution and simulation will be done, an explanation will be given upon the steady state conditions under which deployment of the model will take place, such that the variables can be set appropriately afterwards.

Recall figure 5:

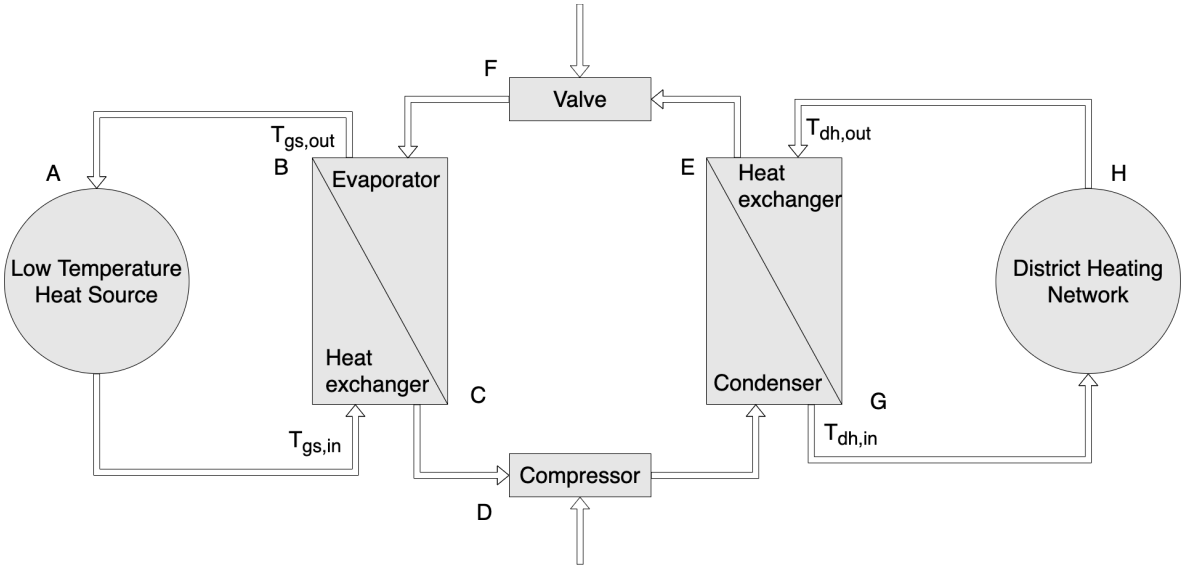

Fig 5: Schematic system model

For which we will first explore components A,B,G and H to investigate what the heat pump should be capable of in practice. Or, in other words, how much heat should be delivered by source A, converted by the heat pump through heat exchangers B and G, and delivered to goal H.

For components H and G, the nominal flow rate of the water supplied by the DH-system in the Saanich case is 25 kg/s, having a temperature of 40°C. The temperature of the flow delivered to the DH-system 50°C after flowing through the heat pump heat exchanger. This is confirmed by Østergaard and Andersen (2016) who explain that the minimum temperature delivery for consumer use should be in between 45°C and 55°C.

The low temperature heat source in the district heating system in Saanich delivers effluent water of a swimming pool facility, which varies between 12°C and 21°C approximately, and has a mass flow of 20 kg/s. For simulation purposes we will assume that the temperature of this flow is 16.5°C. After delivering heat to the evaporator, the temperature of the flow coming from the low temperature heat source usually is 5°C decreased.

From a general energy balance perspective, the following holds for a heat pump system (Vargas and Parise (1994)):

$$\dot{Q}_{evaporator} + \dot{W}_{compressor} = \dot{Q}_{condenser} \tag{49}$$

The valve is left out in this equation, since it does not add work or energy to the fluid. For both the condenser and evaporator, the rate of heat transfer to the district heating system and from the low temperature source, Newton's law of cooling can be applied (Cengel (2008)):

$$\dot{Q} = \dot{m} c_p (T_e - T_{in}) \tag{50}$$

When taking the mass flow and specific heat of water aiming to increase the temperature 10 °C, it turns out that the heat transfer rate from the condenser to the DH-sytem in the Saanich case is equal to 1050kW. Similarly, the heat transfer rate from the low temperature to the evaporator then equals 420 kW. This entails that the total work applied by the compressor then should be 630 kW.

In order to carry out a simulation with the model $F(x) = f(x) + G(x)u.$ with equations 47 and 46, all variables should be set to see how the systems states will develop. In order to do so, the physical properties from Duquette et al. (2016) are used for the length of the tubes and the system configuration of the district heating system and the ground heat source. For the heat pump and transfer properties, values from Vargas and Parise (1994) and He (1996) are extrapolated to the case of Duquette et al. (2016):

Variable	**Value**	**Reference**
L_1	45 m	Duquette et al. (2016)
γ	0.5	Vargas and Parise (1994)
D_{dh}	0.286 m	Duquette et al. (2016)
D_i	0.200 m	Duquette et al. (2016)
A_{dh}	40.43 m^2	$= \pi L_1 D_{dh}$
α_i	3518 W/m^2	He (1996), α_{i2}
α_{dh}	215.77 W/m^2	He (1996), α_{i3}
ρ_{wall}	2702 kg/m^3	Cengel (2008)
$C_{p,wall}$	903 $J/kg \cdot K$	Cengel (2008)
$C_{p,water}$	4200 $J/kg \cdot K$	Cengel (2008)
D_{gs}	0.193 m	Duquette et al. (2016)
L_2	80 m	Duquette et al. (2016)
A_{gs}	24.25 m^2	$= \pi L_2 D_{gs}$
α_{gs}	215.77 W/m^2	He (1996) , α_{i3}

Tab. 1: Heat transfer variables

Similarly, initial values for the state variables are chosen based on literature: the initial states for the temperatures are corresponding to the values of the Saanich case, and the values for the pressures are taken from the operating point of the refrigeration system of Vargas and Parise (1994):

Variable	**Value**	**Reference**
$P_e(0)$	200 kPa	Vargas and Parise (1994)
$T_{w,dh}(0)$	40°C	Duquette et al. (2016)
$T_{dh}(0)$	40°C	Duquette et al. (2016)
$P_c(0)$	1600 kPa	Vargas and Parise (1994)
$T_{w,gs}(0)$	16.5°C	Duquette et al. (2016)
$T_{gs}(0)$	16.5°C	Duquette et al. (2016)

Tab. 2: Initial values state variables

Whenever considering these initial states and the dimensions of the tubes and pipes, the compressor and valve needs to be chosen such that they can handle the flows that are required to deliver the required heat to the DH-system. The refrigerant transfers heat during its phase change in the condenser, and therefore the heat transfer rate from the refrigerant to the wall connecting it to the district heating system can be expressed as (Cengel (2008)):

$$\dot{Q} = \dot{m} h_{fg} \tag{51}$$

Assuming a steady state pressure of 1600 kPa in the condenser (the pressure in the condenser according to Vargas and Parise (1994)), the enthalpy of vaporization of the refrigerant is 141.93 kJ/kg (h_{fg}). This entails that for a heat transfer rate of 1050 kW, a mass flow of 7.4 kg/s is required to to heat up the water in the DH-system (= 0.089 m^3/s). Similarly, a power of 420 kW should be delivered by the low-temperature heat source. Taking a steady-state pressure of 200 kPa, the enthalpy of vaporization equals 206.03 kJ/kg. This implies that the mass flow going through the expansion valve to the evaporator is equal to $2.08kg/s$ (= 0.002 m^3/s).

The compressor and expansion valve should be able to deal with this flows. Hence, as compressor for the centralized district heating system, a industrial compressor (model AWD 4510) from Atlascopo is chosen (Atlascopo (2022)), being able to pump 4510 m^3/h (equal to $1.25m^3/s$), at a full speed of 735 rpm. For the valve, an opening of 0.108 m is chosen, able to let through $0.028m^3$ of refrigerant per second (Extrapolation of model 2028/M12S09 of the handbook for expansion valves (Castel (2021))).

Thus, for the compressor and valve the following initial values are chosen:

Variable	**Value**	**Reference**
V_c	0.1132 m^3	Vargas and Parise (1994), adjusted according to (Atlascopo (2022))
η	0.8	Vargas and Parise (1994)
n	1.5	Vargas and Parise (1994)
C_v	0.05	(Vargas and Parise (1994)) adjusted according to (Castel (2021)).

Tab. 3: Compressor and valve properties

And for the input variables the following initial values are chosen:

Variable	**Value**	**Reference**
$\omega(0)$	12 rev/s	Atlascopo (2022)
$A_v(0)$	0.108 m^2	Castel (2021)
$m_{dh,in}(0)$	25 kg/s	Duquette et al. (2016)
$m_{gs,in}(0)$	20 kg/s	Duquette et al. (2016)

Tab. 4: Initial control inputs

Now that we have defined all variables, a simulation can be performed to investigate the dynamic behavior of the system.

5.3 Simulation

Hence, to investigate the system behavior and to explore equilibria an open loop simulation is carried out, with the introduced initial values for the states. `MATLAB` solver `ODE45` will be used to numerically compute the system of equations $F(x, u)$. `ODE45` is based on an explicit Runge-Kutta formula, and is a single-step solver, which computes $\mathrm{y}(t_n)$ solely on basis of $\mathrm{y}(t_{n-1})$ (Dormand and Prince (1980)). The solver integrates the system of differential equations $F(x, u)$ from timespan t_0 to t_f. Consequently, every iteration presents a solution array for x. These results will be plotted to investigate how the system develops.

As explained, for the initial states the values of table 2 and 4 are used. Hence the following vectors are the initial states and inputs:

$$x_0 = [1600 \quad 40 \quad 40 \quad 200 \quad 16.5 \quad 16.5]^T \qquad u = [12 \quad 0.1 \quad 25 \quad 20]^T \tag{52}$$

With $t_{range} = [0 \qquad 5000]$, results in the following plot for x_1 and x_4.

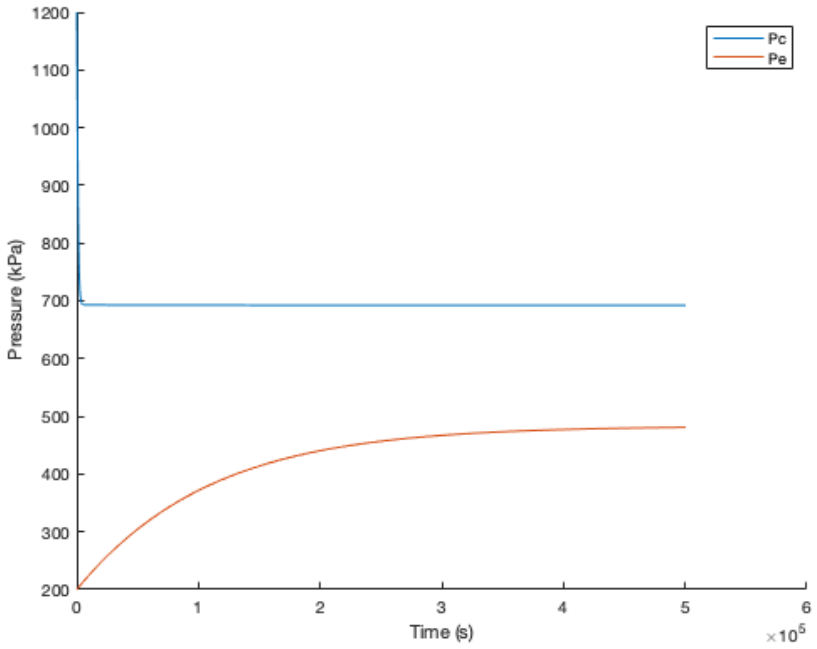

Fig. 14: Evolution of the condenser and evaporator pressures for an open loop simulation

As can be seen, the system stabilizes around $P_{cond} = 700$ and $P_{evap} = 483$. The corresponding wall and flow temperatures of $\dot{m}_{dh}$ and $\dot{m}_{gs}$ are shown in figure 15.

It can be seen that only the initial pressure state is causing a significant temperature difference for the wall, and for the flows. However, when the system stabilizes around $P_{cond} = 700$ kPa and $P_{evap} = 483$ kPa, $T_{w,dh}, T_{dh}, T_{w,gs}$ and T_{gs} converge to the evaporation temperatures for the specific phases at those pressure. Since the pressure states are partly determined by the environment temperatures, the steady-state of the system converges closely to values of T_{in} for both the district heating system and the low temperature heat source.

Hence, now that we have seen that the system converges to steady-state values for the states, we will linearize the system around this equilibrium in order to make controller design possible.

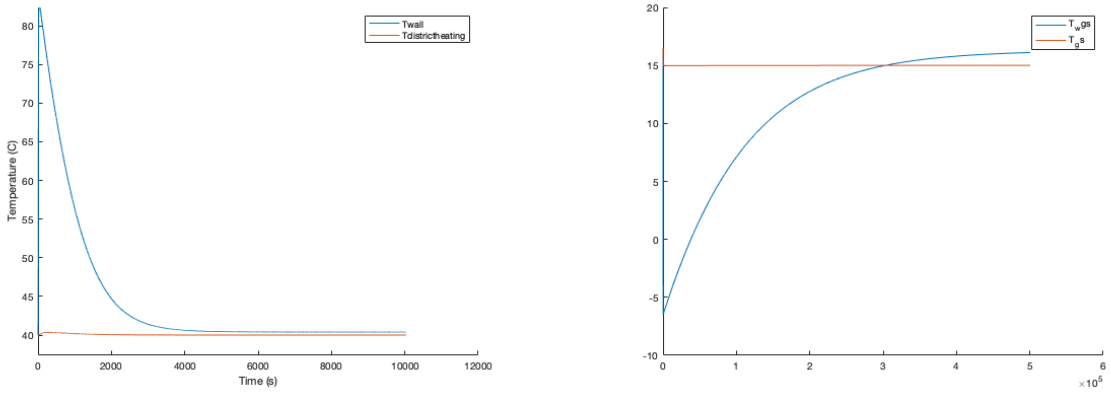

Fig. 15: Open loop temperatures of wall and flows of district heating and heat source

Afterwards, state feedback will be designed in order to investigate whether the system can be manipulated for district heating purposes.

5.4 Jacobian Linearization

The system will be linearized in order to study the local behavior of the system and to overcome the difficult non-linearities. Consider the system:

$$\frac{dx}{dt} = f(x) + G(x)u, \qquad x \in \mathbb{R}^n, \qquad u \in \mathbb{R}^n \tag{53}$$

In which $[x_1 \dots x_6]^T$ are the states for the condenser and evaporator, and $[u_1 \dots u_4]^T$ are the inputs as previously formulated. The Jacobian matrix of x is the matrix of partial derivatives:

$$J(x_1, \dots, x_6) = \begin{bmatrix} \frac{\partial f_1}{\partial x_1} & \cdots & \frac{\partial f_1}{\partial x_6} \\ \vdots & \ddots & \vdots \\ \frac{\partial f_6}{\partial x_1} & \cdots & \frac{\partial f_6}{\partial x_6} \end{bmatrix} \tag{54}$$

Which can be applied on both $f(\bar{x})$ and $g(\bar{x},\bar{u})$u, in which:

$$\bar{x} = \begin{bmatrix} \bar{x}_1 \\ \bar{x}_2 \\ \bar{x}_3 \\ \bar{x}_4 \\ \bar{x}_5 \\ \bar{x}_6 \end{bmatrix} = \begin{bmatrix} 700 \\ 40 \\ 40 \\ 483 \\ 15 \\ 15 \end{bmatrix} \tag{55}$$

$$\bar{u} = \begin{bmatrix} \bar{u}_1 \\ \bar{u}_2 \\ \bar{u}_3 \\ \bar{u}_4 \end{bmatrix} = \begin{bmatrix} 12 \\ 0.01 \\ 25 \\ 20 \end{bmatrix} \tag{56}$$

This results in the following system matrix J for $f(\bar{x})$:

$$J(f(\bar{x})) = \begin{bmatrix} -0.5953 & 5.692 & 0 & 0 & 0 & 0 \\ 6.58 & -82.59 & 20.93 & 0 & 0 & 0 \\ 0 & 0.01 & -0.01 & 0 & 0 & 0 \\ 0 & 0 & 0 & -0.034 & 0.40 & 0 \\ 0 & 0 & 0 & 5.29 & -63.41 & 1.75 \\ 0 & 0 & 0 & 0 & 0.0011 & -1.0011 \end{bmatrix} \tag{57}$$

and for $g(\bar{x})\bar{u}$:

$$J(g(\bar{x}, \bar{u})) = \begin{bmatrix} 0.0002 & 0.4960 & 0 & 0 \\ 0 & 0 & 0 & 0 \\ 0 & 0 & 0.2446 & 0 \\ 0.0013 & -0.0522 & 0 & 0 \\ 0 & 0 & 0 & 0 \\ 0 & 0 & 0 & 0.1468 \end{bmatrix} \tag{58}$$

For $J(f(\bar{x}))$, the behavior of the system can be described by its eigenvalues. Given the system matrix $f(x) \in \mathbb{R}^{n \cdot n}$, v is an eigenvector of $f(x)$ with eigenvalues λ such that (Åström and Murray (2012)):

$$Av = \lambda v \tag{59}$$

Consequently, this results in the following eigenvalues for the system $f(x)$:

$$\lambda_{f(\bar{x})} = \begin{bmatrix} -83.04 \\ -0.06 \\ 0.00 \\ -63.45 \\ 0.00 \\ -0.002 \end{bmatrix} \tag{60}$$

Since these values are negative real numbers, the system is stable. This is line with how the system develops in figure 14: converging towards a stable equilibrium.

Subsequently, the linearized system gives the opportunity to design a controller for the system. Unless that non-linear dynamics are not taken into account, it provides detail in how the model could be executed in a larger district heating context in further research.

5.5 State Feedback

In order to design the dynamics of the system and to reach desired states, a state space controller is designed for the linearized system. Consider the linearized model:

$$\bar{F}(\bar{x}, \bar{u}) = J(f(\bar{x})) + J(g(\bar{x}, \bar{u}))u \tag{61}$$

Which can be described as a linear state space system in the following way:

$$\dot{x} = Ax + Bu \tag{62}$$

$$y = Cx + Du \tag{63}$$

In which A and B are the linearized matrices $J(f(\bar{x}))$ and $J(g(\bar{x}, \bar{u}))$. C is the sensor matrix, and D the feedforward matrix. However, for matrix C we do not know whether we can measure all states. A solution for this would be to design an observer or output regulator. Due to time constraints, we will assume that all states can be measured nevertheless and continue our feedback design. D is equal to zero, since the control signal is not influencing the output directly.

First, to apply state feedback to the dynamical system, it needs to be defined that the system is controllable: it needs to have the ability to reach the origin and an arbitrary state. For the system $\dot{x}$ the controllability matrix is given by:

$$R = \begin{bmatrix} B & AB & A^2B & ... & A^{n-1}B \end{bmatrix} \tag{64}$$

where A is an n-by-n matrix, B is an n-by-m matrix, and R has n rows and nm columns.

The system is controllable if the the controllability matrix has full rank n. Carried out with `MATLAB` command `cntrb(A,B)`, it is determined that the contollability matrix R has rank 6, making the matrix *full rank*. Hence, the system is controllable (Kalman et al. (1963)).

Accordingly, the control system that will be designed, making use of state feedback, is shown in figure 16:

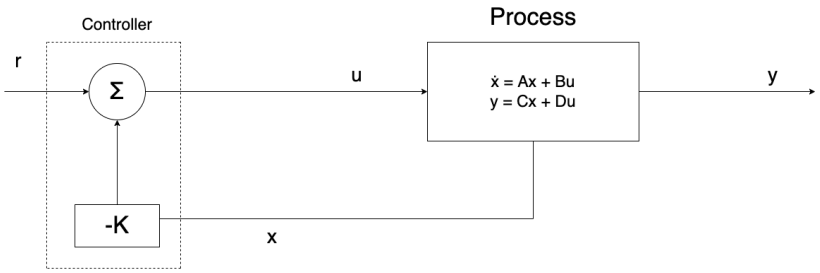

Fig. 16: Feedback control system with state feedback

In this system, the controller uses the system states x and reference input r to steer the process by input u. The goal of the feedback controller is to regulate the output of the system y such that it tracks the reference input and uncertain dynamics in the process. For the linear system described in equations 62 and 63, the feedback can be written as:

$$u = -Kx \tag{65}$$

The closed loop system in figure 16 is then represented by:

$$\frac{dx}{dt} = (A - BK)x \tag{66}$$

In which the feedback gain K needs to be assigned such that the closed loop system has the characteristic polynomial:

$$p(s) = s^n + p_1 s^{n-1} + \ldots + p_{n-1}s + p_n \tag{67}$$

Which is also known as the *pole placement problem* or *eigenvalue assignment problem* (Åström and Murray (2012)). This can be solved by using `MATLAB` command `place`, which computes a gain matrix K such that the state feedback u places the closed-loop poles at the locations p. With the arbitrarily assigned poles

$$p = \begin{bmatrix} -1 & -1 & -1 & -5 & -5 & -5 \end{bmatrix} \tag{68}$$

The resulting gain matrix K is:

$$K = \begin{bmatrix} -0.0023 & 0.0734 & -0.0186 & -0.3906 & 4.6935 & -0.1317 \\ -0.0001 & 0.0018 & -0.0005 & 0.0001 & -0.0018 & 0.0001 \\ -0.0010 & 0.0113 & -0.0028 & -0.0000 & 0.0000 & 0.0000 \\ 0.0000 & 0.0000 & 0.0000 & -0.0012 & 0.0140 & -0.0003 \end{bmatrix} \cdot 10^5 \tag{69}$$

Consequently, this entails that the eigenvalues of feedback system $A - BK$ should be where the poles have been placed. Or, in other words, the eigenvalues of the feedback system should match the entries of p (Kautsky et al. (1985)). This results in the following eigenvalues for the feedback system, corresponding to the poles p.

$$\lambda = \begin{bmatrix} -1 \\ -1 \\ -1 \\ -5 \\ -5 \\ -5 \end{bmatrix} \tag{70}$$

Hence, the physics-based model for the heat pump is suitable to use for control purposes.

6 Discussion

Now that the physics-based model has been subject of simulation and control design, there can be reflected on the conducted research. The aim of this research was to deliver an physics-based mathematical model of a heat pump, suitable to integrate in district heating context. Hence, in this chapter I will discuss and further interpret this. First, I will reflect on the contributions of this research (section 6.1). Secondly, I will discuss the limitations of this research (section 6.2). Finally, I will provide a specific path that can be pursued in further research, by introducing some preliminary findings on a port-hamiltonian perspective on this thesis (section 6.3).

6.1 Contributions

The main contribution of this thesis is the detailed model developed in chapter 4. The physics of the heat pump cycle were thoroughly investigated by means of Vargas and Parise (1994) and He (1996), combining and simplifying both approaches were possible. This resulted in both a modular model describing the four components of the heat pump cycle separately, as well as an aggregated model describing the heat pump dynamics in two state equations.

The developed model has additional value in comparison to available heat pump models of Vargas and Parise (1994), He (1996), B.P. Rasmussen (2006) and Zhang et al. (2014). Particularly, since the state equations and physical dynamics are aggregated and coupled. Additionally, the number of state variables and non-linear equations of the developed model is significantly reduced in comparison to those four available refrigeration models. Besides, the simplicity, uniformity and flexibility of the developed model are also increased with respect to available literature. For instance, instead of focusing on a specific case like automotive air-conditioning (Zhang et al. (2014)), the developed model is suitable for application is various cases.

The choices made for simplification during the modeling procedure were supported by having discussed multiple physical processes elaborately. However, by doing so, it left open the opportunity to obtain a more detailed model by pursuing the conducted discussions. For instance, for the compressor a brief introduction of some alternative modeling options were introduced, whereafter a particular choice was made. Besides, the introduction upon energy balances and the Gibbs and Maxwell equations made it possible to choose one specific state variable (pressure) according to which the entire refrigeration dynamics could be modeled. This has provided a profound physical base for the final mathematical model.

Additionally, the physical model has been used for simulation and control purposes. By implementing it in a particular DH-case and linearizing the model as such, it has been shown that the model is stable and suitable for further control system design. A first contribution has been made by design a state feedback controller by a pole placement procedure.

All together, the conducted research contributes to the DH-modeling of Machado et al. (2021), Schiffer and Krishna (2021), by presenting an alternative for the heat pump cycle of Kim et al. (2014). The level of physical detail was increased by the developed model, but still maintained control inputs and variables that are already present in DH-modeling. This ensures that it should be possible in future research to couple the heat pump model in DH-context.

6.2 Limitations

However, next to the contribution of the developed physical model to current literature, there are some limitations on it.

To start, the choice for pressure as state variable for the refrigerant had some consequences. Unless that it is advantageous for the simplicity of the model, it limits the understanding of the dynamics. For instance, He (1996) introduces enthalpy as state variable, which delivers more detail of the refrigerant dynamics in the condenser and evaporator. If we recap figure 8 (p.16, the Temperature-Entropy and Pressure-Enthalpy diagrams), it can be seen that the enthalpy is the changing variable in the condenser and evaporator. But in this research, the enthalpy development is only estimated based on the uniformity of pressure. The averaged polynomial estimation delivers a method to simplify the model based on pressure development, but looses detail if it comes to enthalpy properties throughout the system.

Likewise, it could have been decided to capture the dynamics of the heat pump cycle in terms of entropy (having in mind the graphs of figure (8, p.16). This would have opened up the opportunity to gain more detailed insights in the refrigerant dynamics in the condenser and evaporator. Specifically, it would have delivered a perspective through which the heat pump dynamics could have been interpreted from a port-hamiltonian perspective (van der Schaft (2021), Villalobos (2020)). This could in particular have been useful to couple the heat pump model to the port-hamiltonian DH-models of Machado et al. (2021) and Schiffer and Krishna (2021). In section 6.3 I will provide some brief insights in how this alternative can be developed in future research, reflecting on the current state of port-hamiltonian thermodynamic systems.

On a more detailed level, the obtained model has some limitations as well. First, improvements could have been made in obtaining a linearized model suitable for control design. For instance, the search for an adequate equilibrium point could have been done in more detail by considering a larger range of system properties and operations. This potentially could have delivered a feasible equilibrium for the forced equilibria of Simpson-Porco (2018) as well, increasing the possibilities for model validation through equilibrum computation by different methods. A second improvement for this research, is that a specific case for centralized district heating was taken into consideration, whilst for individual producers as Schiffer and Machado propose, a heat pump could exhibit different properties. Pressure development within the heat pump cycle could have been validated by investigating different cases, and some closed loop stability analysis would have verified the obtained results for the equilibrium states. Additionally, implementing some experimental values and validating this with conducted research could have improved the accuracy of the model He (1996). Third, comparing the developed model with the initial approaches of Vargas and He, it could also be stated that the dynamics inside the evaporator and condenser tubes could have been simulated and discretized in more detail. For instance, the influence of the different phases of the refrigerant mixing up and influencing each other, is not taken into account. Specifically, since a lumped-parameter approach was undertaken, the different phases were taken into account as being in different compartments, whereas they actually mix up. By taking into account the fluid dynamics and thermal properties of mixed fluids into account, a more detailed account could have been given of the heat conduction process and the mass flow properties (Cengel et al. (2019)). Nevertheless, for integration in district heating purposes, it needs to be kept in mind that with developing more detail, the model should maintain its simplicity for simulation and control

purposes. A fourth improvement could have been made regarding further coupling with the district heating network: the heat pump model should be coupled with a PMSM (Schiffer and Krishna (2021), Kim et al. (2014)). Such a motor can be described in the following way in the *dq*-frame (Ortega et al. (2018)):

$$J\frac{d\omega}{dt} = -R_m\omega + n_p[(L_d - L_q)i_d i_q + \Phi i_q - \tau_l] \tag{71}$$

Where i_d and i_q are input currents, L_d and L_q stator inductances, $\frac{2n_p}{3}$ the number of pole pairs, Φ is the emf back constant and R_m the viscous friction coefficient. If this equation had been worked further out, with the corresponding differential equations for the input currents, one could have obtained a much more detailed understanding about the conversion from electric to thermal energy. An example is given by Vargas and Parise (1994), who proposes a momentum balance over the motor-compressor work, and applies control on a reference voltage for the compressor. Similarly, Kim provides a detailed description of an induction motor to carry out the transient response analysis. This was not taken into account in this research.

Finally, the integration of the heat pump model into a district heating case was not yet researched elaborately. The scope was limited to the heat pump, and therefore implications for DH-systems were not yet taken into account. For instance, it could be researched what the influence of a heat pump is on low voltage networks (Schiffer and Krishna (2021)) and on network efficiency as a whole. For instance, one could carry out an overarching simulation to investigate how much energy savings could be done in combination with RES (Fischer et al. (2017)). Or, if different demands are imposed upon the system, it could be analyzed what the Coefficient of Performance of the coupled heat pump model could be (Madani et al. (2011)). Another way to integrate the model in a larger context, would be to use both air and a ground heat source for heating the evaporator and to investigate how the heat pump efficiency would differ accordingly.

6.3 Further Research: An Hamiltonian Perspective

As already pointed out, it could have been decided during the modeling procedure in this research to take the entropy as state variable for the different components in order to formulate a port-hamiltonian description of the heat pump. However, this would have increased the complexity of the modeling procedure significantly. In current research, port-hamiltonian systems are a novel way of describing thermodynamic system (van der Schaft (2021), Ramirez et al. (2013), Lohmayer et al. (2021)) and hence it would have been too complex and comprehensive to develop this in full detail in this thesis. Nevertheless, it would still be an opportunity to further develop the acquired heat pump model from a port-hamiltonian perspective. This would have led to a different physical interpretation of the heat pump model, and hence would be an alternative to the model developed in this thesis. Unless that it is beyond the primary scope of this research, I will provide some preliminary insights for starting further research in the following paragraphs. For readability purposes, the mathematical definitions and computations of the port-hamiltonian approach are not given in this section, but in Appendix III.

Hamiltonian Systems are a way to model complex physical systems, describing the sum of the total energy in the system. For mechanical systems, for instance, this is defined as the the potential plus the kinetic energy. Energy serves as the *lingua franca* of multi-domain systems, therefore the port-hamiltonian approach can provide a modeling approach in which systems from different physical domains can be coupled (Lohmayer et al. (2021), van der Schaft (2006)). This might be useful for the heat pump model in particular, since it needs to be integrated in a larger multi-energy DH-system.

A specific class of hamiltonian systems are the port-hamiltonian systems, which can be described by network modelling of energy-conserving lumped-parameter physical systems with independent storage elements (Ortega et al. (1980)). The framework of port-hamiltonian system (PHS) generally arise from the first principle of the thermodynamics (the principle of conservation of energy), being able to couple complex multiphysical systems. The port-hamiltonian system theory formalizes the basic interconnection laws of networks together with the power preserving energy-storing elements by a geometric structure, using the Hamiltonian function as the total energy of the system. The input-state-output representation of a finite dimensional port-hamiltonian system is shown by equation (84) in Appendix III (van der Schaft (2006)).

To apply a the port-hamiltonian structure to a thermodynamic system, Villalobos et al. (2020) suggests that the port Hamiltonian system framework should be extended to an *Irreversible port hamiltonian system (IPHS)*, capturing the concept of irreversibility. In this framework, the second principle of thermodynamics is taken into account as well: the irreversible creation of entropy. The definition of an IPHS is shown by equation 86 in Appendix III.

An IPHS-description of a thermodynamic system uses the state variable *entropy*. The challenge for future research following on this thesis is to transform the model such that all components of the heat pump can be described by that state. If this is done, all components can be coupled afterwards to obtain a full IPHS formulation of the heat pump. This model can then be used in the district heating modelling of Machado et al. (2021) and Schiffer and Krishna (2021).

Accordingly, I will deliver some preliminary insights on how the heat pump cycle can be described from the second principle of thermodynamics. Instead of viewing the dynamics of the refrigerant from its pressure state and the flow of the district heating system from its temperature state, entropy needs to describe the energy in the subsystems.

Hence, we will shortly recap section 3.3, in which the state variables for the heat pump cycle were defined. Recalling equation 4:

$$TdS = dU + Pdv \tag{72}$$

In which the total energy is defined as the change in entropy with uniform temperature, minus the change in volume at uniform pressure:

$$dE = TdS - PdV \tag{73}$$

Or in other words, this corresponds to the Maxwell relation which describes the change in entropy in terms of change in volume (Cengel et al. (2019)):

$$\left(\frac{\delta s}{\delta P}\right)_T = -\left(\frac{\delta v}{\delta T}\right)_P \tag{74}$$

This Maxwell relation is in particular useful since the refrigerant in the condenser and evaporator is assumed to have uniform pressure and temperature. Van der Schaft (2021) shows that this can be rewritten to an entropy representation:

$$dS = \frac{1}{T}dE + \frac{P}{T}dV \tag{75}$$

Accordingly, equation (75) can be applied on both the condenser and evaporator as shown in figure 10 (p.24). Van der Schaft (2021) delivers a scheme which might be of particular use for this application: a port-hamiltonian representation of a heat exchanger, shown in figure 17. This heat exchanger is similar to the heat exchangers in the heat pump model, and hence the port-hamiltonian formulation of the heat exchanger can deliver a preview of what a IPHS heat pump model would look like.

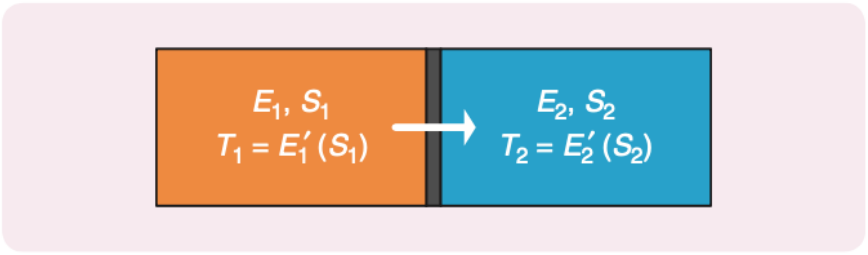

Fig. 17: A schematic representation of a heat exchanger (van der Schaft (2006))

With this figure, (van der Schaft (2021)) shows that for a heat exchanger with one substance at either side, the extensive variables are S1, S2 (entropies of the two compartments), and E (total internal energy). This figure can be combined with the mathematical interpretation Ramirez et al. (2013) provides for an IPHS heat exchanger. Afterwards, the method can be applied on the condenser and evaporator to develop an IPHS formulation for them. This is further elaborated in Appendix III.

However, in order to fit the approach of Ramirez et al. (2013) and van der Schaft (2021) to the heat pump cycle of this thesis, some remarks need to be taken into account. Since the substance in the heat exchangers of the heat pump cycle consists of both gas and liquid, the entropy also is a combination of the entropy of both phases (see Appendix II). Hence, the entropy balance for both the fluid and liquid need to be taken into account in formulating an IPHS: instead of viewing both sides a having one phase, they need to be separated into several compartments (explained in section 4.1, p.20. For a detailed IPHS-description of mixed substances, see (Bansal et al. (2021))). This is different from what (van der Schaft (2021)) and (Ramirez et al. (2013)) are doing, since in their approach they only consider a conventional heat exchanger with one phase at either side. Therefore, their system formulation will be adjusted in order to obtain the desired IPHS-formulation for both the condenser and evaporator. Instead of viewing the energy of the left side of figure 17 as $E_1(S1)$, it will be

viewed as a mixed substance. This results in a transformation from equation 89 to 90, shown in Appendix III.

For the valve and compressor an energy-representation needs to be found likewise in future research. The valve is straightforward to model, since it is an isenthalpic device in which the total energies of the fluid remain constant. Unless that during a throttling process, internal and flow energies can be converted to each other, the sum of it remains constant (Cengel (2008)). Hence, the valve can be ignored when formulating the heat pump cycle in port-hamiltonian form. For the compressor, equation 32 (p.27) gives a good first impression of what could be a suitable way to represent the energy dynamics of the compressor itself. As can be seen in figure 8, the entropy during a compression process is constant. Hence, it needs to be researched how and if the pressure and volumetric changes can be expressed in an entropy-based representation.

Formulating the heat pump cycle in terms of an port-hamiltonian framework is a promising path for future research. In this previewing discussion it was tried to deliver some first insights by setting a different state variable and applying this to the evaporator and condenser. However, further development and validation for this part are required to finally come up with a full IPHS description suitable for DH-integration.

7 Conclusion

Heat pumps can be of decisive value when it comes to reducing CO2-emissions in future energy systems. Specifically, these devices offer flexibility in transforming electric energy into thermal energy. In this thesis, I aimed to deliver a physical understanding of this process, suitable for integration in DH-systems. In state-of-the-art literature, there was room to develop a dynamical model of heat pump. Specifically, a model was required that was able to capture the physical processes and complexity of the refrigeration cycle, but that maintained the simplicity and uniformity to couple it into larger contexts. The model developed in this thesis aimed to satisfy these requirements.

Accordingly, I have discussed the basic thermodynamic processes that are laying at the foundation of this refrigeration cycle. By doing so, it was possible to decide upon state variables and to write down its dynamics based on it. Combining the choice upon the state variable pressure with existing heat pump models, eventually delivered a dynamical model that was suitable for control purposes. As was shown in chapter 5, the dynamical model exhibits properties appropriate for case-specific simulation and control design. Additionally, the detailed physical framework has delivered the opportunity to reflect upon the modeling procedure, and provides some brief preliminary thoughts upon a port-hamiltonian systems approach.

Concluding, the objective of the performed research was to deliver a dynamical model with an advanced level of detail regarding the physical working of the heat pump, able to integrate in a DH-sytem. With the results delivered in this thesis, I aimed to achieve this goal. In particular, I hope that with the developed model, the possibilities for heat pump application in modern energy systems will increase, such that they can be transformed towards a carbon-neutral future.

References

A.S.H.R.A.E. (2008). *Handbook, HVAC Systems and Equipment (SI)*. ASHREA Inc.

Atlascopo (2022). General catalog for compressor air, gas and vacuum solutions. *https://www.atlascopco.com/content/dam/atlas-copco/compressor-technique/industrial-air/documents/brochures/CT%20Catalogue_ Full.pdf*, (URL Accessed: 12-01-2022).

Baniasadi, A., Habibi, D., Bass, O., and Masoum, M. A. (2019). Optimal real-time residential thermal energy management for peak-load shifting with experimental verification. *IEEE Transactions on Smart Grid*, pages 5587–5599.

Bansal, H., Schulze, P., Abbasi, M. H., Zwart, H., Iapichino, L., Schilders, W. H., and van de Wouw, N. (2021). Port-hamiltonian formulation of two-phase flow models. *Systems Control Letters*, 149(104881).

B.P. Rasmussen, A. A. (2006). Dynamic modeling and advanced control of air conditioning and refrigeration systems. *Air Conditioning and Refrigeration Systems*.

Cao, Y., Wei, W., Wang, J., Mei, S., Shafie-khah, M., and Catalao, J. P. (2020). Capacity planning of energy hub in multi-carrier energy networks: A data-driven robust stochastic programming approach. *IEEE Transactions on Sustainable Energy*, 11(1):3–14.

Castel (2021). *Expansion Valves for Refrigeration Systems*. Castel ((ed. 001-VE-ENG)).

Cengel, Y. A. (2008). *Introduction to Thermodynamics and Heat Transfer*. New York: McGraw-Hill.

Cengel, Y. A., Boles, M. A., and Kanoglu, M. (2019). *Thermodynamics: An Engineering Approach*. [ninth edition], New York: McGraw-Hill.

Chua, K. J., Chou, S. K., and Yang, W. M. (2010). Advances in heat pump systems: A review. *Applied Energy*, 87:3611–3624.

Cleland, A. (1992). Polynomial curve-fits for refrigerant thermodynamic properties: extension to include r134a. *International journal of refrigeration*, 17(4):245–259.

Dormand, J. R. and Prince, P. J. (1980). A family of embedded runge-kutta formulae. *Journal of computational and applied mathematics*, 6(1):19–26.

Duquette, J., Rowe, A., and Wild, P. (2016). Thermal performance of a steady state physical pipe model for simulating district heating grids with variable flow. *Applied Energy*, 178:383–393.

Fischer, D., Bernhardt, J., Madani, H., and Wittwer, C. (2017). Comparison of control approaches for variable speed air source heat pumps considering time variable electricity prices and pv. *Applied Energy*, 204:93–105.

Fischer, D. and Madani, H. (2017). On heat pumps in smart grids: a review. *Renewable and Sustainable Energy Reviews*, 70:342–357.

Hauschild, S. A., Marheineke, N., Mehrmann, V., Mohring, J.and Badlyan, A. M., Rein, M., and Schmidt, M. (2020). Port-hamiltonian modeling of district heating networks. *Progress in Differential-Algebraic Equations*, II:333–355.

He, X.-D. (1996). *Dynamic Modeling and Multivariable Control of Vapor Compression Cycles in Air Conditioning Systems*. Massachusetts Institute of Technology.

Jayawardhana, B., Ortega, R., Garcia-Canseco, E., and Castanos, F. (2007). Passivity of nonlinear incremental systems: Application to pi stabilization of nonlinear rlc circuits. *Systems Control Letters*, 56(9):618 – 622.

Kalman, R. E., Ho, Y., and Narendra, K. S. (1963). Controllability of linear dynamical systems. *volume 1 of Contributions to Differential Equations*.

Kaushik, S. C., Tyagi, S. K., and Kumar, P. (2017). *Finite Time Thermodynamics of Power and Refrigeration Cycles*. Springer.

Kautsky, J., Nichols, N. K., and Van Dooren, P. (1985). Robust pole assignment in linear state feedback. *International Journal of control*, 41(5):1129–1155.

Kim, Y.-J., Norford, L. K., and Kirtley., J. L. (2014). Modeling and analysis of a variable speed heat pump for frequency regulation through direct load control. *IEEE Transactions on Power Systems*, 30(1):397–408.

Klyapovskiy, S., You, S., Cai, H., and Bindner, H. W. (2018). Integrated planning of a large-scale heat pump in view of heat and power networks. *IEEE Transactions on Industry Applications*, 55(1):5–15.

Li, R., Wei, W., Mei, S., Hu, Q., and Wu, Q. (2019). Participation of an energy hub in electricy and heat distribution markets: An mpec approach. *IEEE Transactions on Smart Grid*, 10(4):3641–3653.

Li, W. (2012). Simplified modeling analysis of mass flow characteristics in electronic expansion valve. *Applied Thermal Engineering*, (53):8–12.

Lohmayer, M., Kotyczka, P., and Leyendecker, S. (2021). Exergetic port-hamiltonian systems: modelling basics. *Mathematical and Computer Modelling of Dynamical Systems*, 27(1):489–521.

Lund, H., Werner, S., R., W., Svendsen, S., Thorsen, J. E., Hvelplund, F., and Mathiesen, B. V. (2014). 4th generation district heating (4gdh). integrating smart thermal grids into future sustainable energy systems. *Energy*, 68:1–11.

MacArthur, J. W. and Grald, E. W. (2021). Unsteady compressible two-phase flow model for predicting cyclic heat pump performance and a comparison with experimental data. *Conference paper*.

Machado, J. E., Cucuzzella, M., and Scherpen, J. (2021). Modeling and passivity properties of district heating systems. *Automatica*.

Madani, H., Claesson, J., and Lundqvist, P. (2011). Capacity control in ground source heat pump systems. part i: modeling and simulation. *International Journal of Refrigeration*, 34:1338–1347.

Mahdavi, N. and Braslavsky, J. H. (2020). Modelling and control of ensembles of variable-speed air conditioning loads for demand response. *IEEE Transactions on Smart Grid*, 11(5):4249–4260.

Mathworks (2021). Polyfit: polynomial curve fitting. *https://nl.mathworks.com/help/matlab/ref/polyfit.html*, (URL Accessed: 10-12-2021).

Ndiaye, D. and Bernier, M. (2009). Dynamic model of a hermetic reciprocating compressor in on-off cycling operation. *Applied Thermal Engineering*, pages 792–799.

Nyers, J. and Stoyan, G. (1994). A dynamical model adequate for controlling the evaporator of a heat pump. *International Journal of refrigeration*, 17(2):101–108.

Ortega, R., Monshizadeh, N., Monshizadeh, P., Bazylev, D., and Pyrkin, A. (2018). Permanent magnet synchronous motors are globally asymptotically stabilizable with pi current control. *Automatica*, 98:296–301.

Ortega, R., van der Schaft, A., Maschke, B., and Escobar, G. (1980). Interconnection and damping passivity-based control of port hamiltonian systems. *Journal of computational and applied mathematics*, 6(1):19–26.

Pedersen, T. S., Andersen, P., Nielsen, K. M., Stærmose, H. L., and Pedersen, P. D. (2011). Using heat pump energy storages in the power grid. *IEEE International Conference on Control Applications*, pages 1106–1111.

Péan, T., Costa-Castelló, R., Fuentes, E., and Salom, J. (2019). Experimental testing of variable speed heat pump control strategies for enhancing energy flexibility in buildings. *IEEE access*, 7:37071–37087.

Ramirez, H., Maschke, B., and Sbarbaro, D. (2013). port-hamiltonian systems: A general formulation of irreversible processes with application to the cstr. *Irreversible Chemical Engineering Science*, 89:223–234.

Rasmussen, B., Musser, A., Alleyne, A., Bullard, C., Hrnjak, P., and Miller, N. (2002). A control-oriented model of transcriticai air-conditioning system dynamics. *SAE Transactions*, pages 374–381.

Sadeghi, H., Rashidinejad, M., Moeini-Aghtaie, M., and Abdollahi, A. (2019). The energy hub: An extensive survey on the state-of-the-art. *Applied Thermal Engineering*, 161:114071.

Schiffer, J. and Krishna, A. (2021). A port-hamiltonian approach to modeling an control of an electro-thermal microgrid. *[Conference Paper]*.

Simpson-Porco, J. W. (2018). Equilibrium-independent dissipativity with quadratic supply rates. *IEEE Transactions on Automatic Control*, 64(4):1440–1455.

van der Schaft, A. (2006). Port-hamiltonian systems: an introductory survey. *Proceedings of the international congress of mathematicians.*, 3:1339–1365.

van der Schaft, A. (2021). Classical thermodynamics revisited. *IEEE Control Systems Magazine*, 41(5):32–60.

Vargas, J. and Parise, J. (1994). Simulation in transient regime of a heat pump with closed loop and on-off control. *International Journal of Refrigeration*, 18(4):235–243.

Villalobos, A. (2020). Passivity based control of irreversible port hamiltonian system: and energy shasping plus damping injection approach. *Master Thesis Universidad Tecnica Federico Santa Maria*.

Villalobos, I., Ramírez, H., and Le Gorrec, Y. (2020). Energy shaping plus damping injection of irreversible port hamiltonian systems. *Irreversible Chemical Engineering Science*, 53(2):11539–11544.

Xie, G. and Bansal, P. K. (2000). Dynamic simulation model of a reciprocating compressor in a refrigerator. *International Compressor Engineering Conference*, (1376):19–136.

Zhang, Q., Stockar, S., Canova, M., Hu, H., Liu, Y., and Yuan, L. (2014). Energy-optimal control of an automotive air conditioning system for ancillary load reduction. *IEEE Transactions on Control Systems Technology*, pages 1–14.

Åström, K. J. and Murray, R. M. (2012). *Feedback Systems: An Introduction for Scientists and Engineers*. New Jersey: Princeton University Press.

Østergaard, P. A. and Andersen, A. N. (2016). Booster heat pumps and central heat pumps in district heating. *Applied Energy*, 184:(2016): 1374–1388.

Appendix I

The polynomials which estimate the temperature, enthalpy and density of refrigerant R134a throughout the refrigeration cycle, are the following:

$$T_r(_P) = 1.3008 \cdot 10^{-5} P^2 + 0.0733P - 22.3122 \tag{76}$$

$$T_{r,sh}(_P) = \frac{1}{\eta}(1.3008 \cdot 10^{-5} P^2 + 0.0733P - 22.3122) \tag{77}$$

$$h_l(_P) = -1.5886 \cdot 10^{-5} P^2 + 0.0995P + 21.6127 \tag{78}$$

$$h_g(_P) = -9.9776 \cdot 10^{-6} P^2 + 0.0427P + 237.552 \tag{79}$$

$$h_{sh}(_P) = \frac{1}{\eta}\left(-9.9776 \cdot 10^{-6} P^2 + 0.0427P + 237.552\right) \tag{80}$$

$$\rho_l(_P) = 2.8309 \cdot 10^{-5} P^2 - 0.2431P + 1369 \tag{81}$$

$$\rho_g(_P) = 7.9202 \cdot 10^{-6} P^2 + 0.0376P + 2.6773 \tag{82}$$

$$\rho_{sh}(_P) = \frac{1}{\eta}\left(7.9202 \cdot 10^{-6} P^2 + 0.0376P + 2.6773\right) \tag{83}$$

Appendix II

Saturated refrigerant-134a—Pressure table

		Specific volume, m^3/kg		Internal energy, kJ/kg			Enthalpy, kJ/kg			Entropy, kJ/kg · K		
Press., P kPa	Sat. temp., T_{sat} °C	Sat. liquid, v_f	Sat. vapor, v_g	Sat. liquid, u_f	Evap., u_{fg}	Sat. vapor, u_g	Sat. liquid, h_f	Evap., h_{fg}	Sat. vapor, h_g	Sat. liquid, s_f	Evap., s_{fg}	Sat. vapor, s_g
60	−36.95	0.0007098	0.31121	3.798	205.32	209.12	3.841	223.95	227.79	0.01634	0.94807	0.96441
70	−33.87	0.0007144	0.26929	7.680	203.20	210.88	7.730	222.00	229.73	0.03267	0.92775	0.96042
80	−31.13	0.0007185	0.23753	11.15	201.30	212.46	11.21	220.25	231.46	0.04711	0.90999	0.95710
90	−28.65	0.0007223	0.21263	14.31	199.57	213.88	14.37	218.65	233.02	0.06008	0.89419	0.95427
100	−26.37	0.0007259	0.19254	17.21	197.98	215.19	17.28	217.16	234.44	0.07188	0.87995	0.95183
120	−22.32	0.0007324	0.16212	22.40	195.11	217.51	22.49	214.48	236.97	0.09275	0.85503	0.94779
140	−18.77	0.0007383	0.14014	26.98	192.57	219.54	27.08	212.08	239.16	0.11087	0.83368	0.94456
160	−15.60	0.0007437	0.12348	31.09	190.27	221.35	31.21	209.90	241.11	0.12693	0.81496	0.94190
180	−12.73	0.0007487	0.11041	34.83	188.16	222.99	34.97	207.90	242.86	0.14139	0.79826	0.93965
200	−10.09	0.0007533	0.099867	38.28	186.21	224.48	38.43	206.03	244.46	0.15457	0.78316	0.93773
240	−5.38	0.0007620	0.083897	44.48	182.67	227.14	44.66	202.62	247.28	0.17794	0.75664	0.93458
280	−1.25	0.0007699	0.072352	49.97	179.50	229.46	50.18	199.54	249.72	0.19829	0.73381	0.93210
320	2.46	0.0007772	0.063604	54.92	176.61	231.52	55.16	196.71	251.88	0.21637	0.71369	0.93006
360	5.82	0.0007841	0.056738	59.44	173.94	233.38	59.72	194.08	253.81	0.23270	0.69566	0.92836
400	8.91	0.0007907	0.051201	63.62	171.45	235.07	63.94	191.62	255.55	0.24761	0.67929	0.92691
450	12.46	0.0007985	0.045619	68.45	168.54	237.00	68.81	188.71	257.53	0.26465	0.66069	0.92535
500	15.71	0.0008059	0.041118	72.93	165.82	238.75	73.33	185.98	259.30	0.28023	0.64377	0.92400
550	18.73	0.0008130	0.037408	77.10	163.25	240.35	77.54	183.38	260.92	0.29461	0.62821	0.92282
600	21.55	0.0008199	0.034295	81.02	160.81	241.83	81.51	180.90	262.40	0.30799	0.61378	0.92177
650	24.20	0.0008266	0.031646	84.72	158.48	243.20	85.26	178.51	263.77	0.32051	0.60030	0.92081
700	26.69	0.0008331	0.029361	88.24	156.24	244.48	88.82	176.21	265.03	0.33230	0.58763	0.91994
750	29.06	0.0008395	0.027371	91.59	154.08	245.67	92.22	173.98	266.20	0.34345	0.57567	0.91912
800	31.31	0.0008458	0.025621	94.79	152.00	246.79	95.47	171.82	267.29	0.35404	0.56431	0.91835
850	33.45	0.0008520	0.024069	97.87	149.98	247.85	98.60	169.71	268.31	0.36413	0.55349	0.91762
900	35.51	0.0008580	0.022683	100.83	148.01	248.85	101.61	167.66	269.26	0.37377	0.54315	0.91692
950	37.48	0.0008641	0.021438	103.69	146.10	249.79	104.51	165.64	270.15	0.38301	0.53323	0.91624
1000	39.37	0.0008700	0.020313	106.45	144.23	250.68	107.32	163.67	270.99	0.39189	0.52368	0.91558
1200	46.29	0.0008934	0.016715	116.70	137.11	253.81	117.77	156.10	273.87	0.42441	0.48863	0.91303
1400	52.40	0.0009166	0.014107	125.94	130.43	256.37	127.22	148.90	276.12	0.45315	0.45734	0.91050
1600	57.88	0.0009400	0.012123	134.43	124.04	258.47	135.93	141.93	277.86	0.47911	0.42873	0.90784
1800	62.87	0.0009639	0.010559	142.33	117.83	260.17	144.07	135.11	279.17	0.50294	0.40204	0.90498
2000	67.45	0.0009886	0.009288	149.78	111.73	261.51	151.76	128.33	280.09	0.52509	0.37675	0.90184
2500	77.54	0.0010566	0.006936	166.99	96.47	263.45	169.63	111.16	280.79	0.57531	0.31695	0.89226
3000	86.16	0.0011406	0.005275	183.04	80.22	263.26	186.46	92.63	279.09	0.62118	0.25776	0.87894

Appendix III

Input-state-output representation of a finite dimensional port-hamiltonian system:

$$\dot{x} = [J(x) - R(x)]\frac{\partial H}{\partial x} + g(x)u(t) \tag{84}$$

$$y(t) = g^T(x)\frac{\partial H}{\partial x} \tag{85}$$

Where $x(t) \in \mathbb{R}^n$ is the state space vector $u(t) \in \mathbb{R}^m$ the input of the system, $H(x)$: $\mathbb{R}^n \to \mathbb{R}$ is the Hamiltonian function (which presents the total energy) and $g(x) \in \mathbb{R}^{n\times m}$ is the input map. The matrices $J(x) \in \mathbb{R}^{n\times n}, R(x) \in \mathbb{R}^{n\times n}$ are respectively the structure matrix and dissipation matrix of the system.

An Irreversible port-hamiltonian system representation:

$$\dot{x} = J\left(x, \frac{\partial U}{\partial x}\right)\frac{\partial U}{\partial x} + g\left(x, \frac{\partial U}{\partial x}\right)u \tag{86}$$

$$y(t) = g\left(x, \frac{\partial U}{\partial x}\right)^T\frac{\partial U}{\partial x} \tag{87}$$

Where $x(t) \in \mathbb{R}^n$ is the state space vector $u(t) \in \mathbb{R}^m$ the input of the system, $H(x)$: $\mathbb{R}^n \to \mathbb{R}$ is the Hamiltonian function which is a smooth function of the state x. The structure skew-symmetric matrix is $J = -J^T$ and the input map is g $\in \mathbb{R}^{nxm}$. There exists a smooth entropy function S(x): $\mathbb{R}^n \to \mathbb{R}$.

Preliminary irreversible port-hamiltonian notation

The resulting dynamics of a heat exchanger using entropy as state variables can be described in the following way (Ramirez et al. (2013)):

$$\begin{bmatrix} \dot{S}_1 \\ \dot{S}_2 \end{bmatrix} = \lambda \begin{bmatrix} \frac{T_2(S_2)}{T_1(S_1)} - 1 \\ \frac{T_1(S_1)}{T_2(S_2)} - 1 \end{bmatrix} + \begin{bmatrix} 0 \\ \frac{T_e(t)}{T_2(S_2)} - 1 \end{bmatrix} \tag{88}$$

$$E_1(S_1) = (\gamma)(E_{gas}(S_{gas})) + (1-\gamma)(E_{liquid}(S_{liquid})) \tag{89}$$

For simplification and unification reasons, we will view the condenser like it has two different volumes, together interacting with the district heating system through heat conduction. Subscript 1 refers to the properties of the gas refrigerant, subscript 2 to the liquid refrigerant, and 3 to the liquid flowing through the district heating system. Summarized, the total entropy in the condenser satisfies:

$$\frac{d}{dt}(S_1 + S_2 + S_3) = \lambda \left(\frac{1}{E_1'(S1)} + \frac{1}{E_2'(S2)} + \frac{1}{E_3'(S3)} \right) (E_3'(S3) - E_2'(S2) - E_1'(S1)) \tag{90}$$

In which λ is equal to Fourier's conduction coefficient for the wall.

Subsequently, (van der Schaft (2021)) states that the change in energy is represented in terms of temperature as intensive variable:

$$T_x = E_x'(S_x) \tag{91}$$

Hence, the dynamics can be written down with state variable entropy for each part, taking into account the void fraction which was introduced earlier on in section 3.1.

$$\begin{bmatrix} (1-\gamma)\dot{S}_1 \\ (\gamma)\dot{S}_2 \\ \dot{S}_3 \end{bmatrix} = \lambda \begin{bmatrix} -\frac{T_1(S_1) + T_2(S_2) - T_3(S_3)}{T_1(S_1)} \\ -\frac{T_1(S_1) + T_2(S_2) - T_3(S_3)}{T_2(S_2)} \\ \frac{T_1(S_1) + T_2(S_2) - T_3(S_3)}{T_3(S_3)} \end{bmatrix} \tag{92}$$

Which can also be written as:

$$\frac{d}{dt}(S_1 + S_2 + S_3) = \lambda \left(\frac{1}{T_1(S1)} + \frac{1}{T_2(S2)} + \frac{1}{T_3(S3)} \right) (T_3(S3) - T_2(S2) - T_1(S1)) \tag{93}$$

Which is equal to:

$$\begin{bmatrix} (1-\gamma)\dot{S}_1 \\ (\gamma)\dot{S}_2 \\ \dot{S}_3 \end{bmatrix} = \lambda \left(\frac{1}{T_1(S1)} + \frac{1}{T_2(S2)} + \frac{1}{T_3(S3)} \right) \begin{bmatrix} 0 & 0 & 1 \\ 0 & 1 & 0 \\ -1 & 0 & 0 \end{bmatrix} \begin{bmatrix} \frac{\partial E}{S_1} \\ \frac{\partial E}{S_2} \\ \frac{\partial E}{S_3} \end{bmatrix} \tag{94}$$

This system can be rewritten in IPHS-form:

$$\dot{x} = R(x,T)JT(x) + g(T)u(t) \tag{95}$$

In which $R(x,T(x)) = \lambda(\frac{1}{T_3} - \frac{1}{T_2} - \frac{1}{T_1})$ and $J = \begin{bmatrix} 0 & 0 & 1 \\ 0 & 1 & 0 \\ -1 & 0 & 0 \end{bmatrix}$

The input map $g(T)u(t)$ is defined by the interaction with the other subsystems. The first input is the gas flow coming from the compressor, which delivers superheated vapor to the condenser. The second one is the flow going through the district heating system. The inputs for the system represented in (92) are:

$$g(T)u(t) = \begin{bmatrix} h_c & 0 & h_{dh} \end{bmatrix} \begin{bmatrix} \frac{T_c(t) - T_1(S_1)}{T_1(S_1)} \\ 0 \\ \frac{T_{dh}(t) - T_3(S_3)}{T_3(S_3)} \end{bmatrix} \tag{96}$$

in which h_c and h_{dh} are the convection coefficients for the flow coming in from the compressor and from the district heating system. For the evaporator equation (90) till (96) can be constructed likewise, but with convection coefficients for the low temperature heat source and valve.